

AD 693452

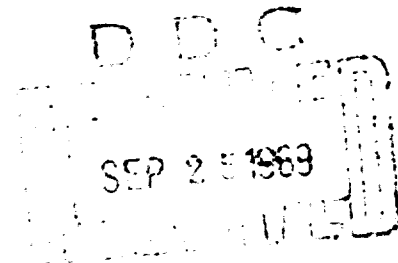
NRL Memorandum Report 2025

A Review of Radar Sea Echo

MERRILL I. SKOLNIK

Radar Division

July 1969



NAVAL RESEARCH LABORATORY
Washington, D.C.

This document has been approved for public release and sale; its distribution is unlimited.

A REVIEW OF RADAR SEA ECHO

Merrill I. Skolnik

ABSTRACT

The radar echo from the sea limits the ability of radar to detect targets. A knowledge of the sea echo is necessary, therefore, for proper design of radars that must detect targets on or over the sea. This report briefly reviews the ocean surface characteristics that affect radar echo and summarizes the present status of knowledge of the sea echo as a function of radar grazing angle, sea state and wind, polarization, frequency and other factors. A plot of σ^0 (radar cross section per unit area) as a function of grazing angle and frequency obtained from an averaged composite of reported data shows that no simple law of frequency dependence should be expected. The attempts made in the past to provide theoretical models describing the sea echo are reviewed and lead up to the presently accepted models of scattering surfaces composed of the larger gravity waves on which are superimposed the smaller capillary waves. The influence of sea echo on radar design is discussed and is considerably different than the usual design restraints imposed by thermal noise. The potential application of radar for oceanographic measurements such as sea state and wind is described.

TABLE OF CONTENTS

1. INTRODUCTION
 2. GRAZING ANGLE
 3. SEA STATE AND WIND
 4. POLARIZATION
 5. FREQUENCY
 6. OTHER FACTORS
 - Rain
 - Contaminants
 - Pulse Length
 - False Alarms
 - Shadowing
 - Fluctuations
 - Doppler
 - Trapping
 7. SEA ECHO THEORY
 8. INFLUENCE ON DESIGN
 - Range Equation for Clutter
 - Polarization Choice
 - Critical Angle and Target Detectability
 - Clutter Matched Filter
 - MTI
 - Decorrelation with Frequency
 - The Selection of σ^0
 9. POTENTIAL OCEANOGRAPHIC APPLICATIONS
- REFERENCES

A REVIEW OF RADAR SEA ECHO*

1. INTRODUCTION

A radar that must detect targets on or near the surface of the sea must cope with the echo returned by the sea itself. The sea echo can be relatively large and in many instances it, rather than receiver noise, limits the detection capability of a radar. Thus, when it is necessary to detect ships, low flying aircraft, navigation buoys, land-sea boundaries and other objects near or in the water, a knowledge of sea echo is important for effective radar design. The character of the sea echo is not only important to the design of radars but it can also be used to obtain a measurement of ocean surface effects of interest to the oceanographer such as surface roughness and wave patterns.

Many measurements of the radar return from the sea have been made by many experimenters. These measurements have been obtained at frequencies ranging from HF to millimeter wavelengths to optical wavelengths and under a variety of conditions. The data covers a wide spread of values but even under supposedly identical conditions there has not always been good agreement among experiments. Part of the large variation of data is due to the difficulty of measuring or describing the sea and the environment. The speed, duration, fetch and direction of the wind at the water surface, the ocean currents, contaminants such as oil, the effects of distant storms that propagate disturbances of the sea with low loss over vast distances, bottom variations, and local weather can all have an effect on sea echo and are difficult to measure, much less control, in field experiments. Furthermore there are the usual difficulties of an accurate calibration needed for an absolute measurement of radar cross section. Calibration is especially difficult for sea echo since it is seldom measured under laboratory-like conditions. The sea echo has also been observed to increase by as much as 10 db in a one minute interval.³¹ These factors, and perhaps others not even known, all result in uncertainty in the data. The radar designer must therefore take account of the variation of data in his design and in the specification of performance.

This report presents representative experimental data regarding sea echo and its variation with radar parameters and sea conditions. Because of the wide spread in the data from experimenter to experimenter or even

*This report is a slightly enlarged version of Chapter 26 of the RADAR HANDBOOK, Edited by M. I. Skolnik, McGraw-Hill Book Co., New York, 1970.

in different runs by the same experimenter, the curves of sea echo should be considered illustrative rather than a firm description applicable to all conditions. The implications on radar design are described and a brief review of existing sea echo theory is given. Although the term sea echo is used almost exclusively here (except in Sec. 8), the terms sea clutter and sea return are also found in the literature.

The sea is a distributed target and the magnitude of the echo depends on the area illuminated by the radar beam. To eliminate the effect of the size of the illuminated patch, sea echo is usually described in terms of the radar cross section per unit area illuminated and is designated $\sigma^0 = \sigma/A$, where σ is the radar cross section and A is the area of the sea illuminated by the radar. At low grazing angles φ , the area A is approximately $R \theta_B (c \tau/2) \sec \varphi$, where R is the range, θ_B is the azimuth beamwidth, c is the velocity of propagation, and τ is the pulse width (Fig. 1). At high grazing angles where the illuminated area is determined only by the antenna beamwidth rather than the pulse width, the area is approximately $R^2 \Omega_B$, where Ω_B is the solid angle of the radar antenna in steradians. The parameter σ^0 is sometimes called the clutter coefficient.

Much of the terminology of the oceanographer used to describe the sea is often unfamiliar to the radar engineer. Some of the more useful terms for the description of sea echo are given below:¹

Wind wave -- A wave resulting from the action of the wind on a water surface. While the wind is acting on it, it is a sea, thereafter, a swell.

Gravity wave -- A wave whose velocity of propagation is controlled primarily by gravity. Water waves of length greater than 2 inches are considered gravity waves.

Capillary wave (also called ripple, capillary ripple) -- A wave whose velocity of propagation is controlled primarily by the surface tension of the liquid in which the wave is traveling. Water waves of length less than one inch are considered to be capillary waves.

Fetch -- 1. (Also called generating area) An area of the sea surface over which seas are generated by a wind having a constant direction and speed. 2. The length of the fetch area, measured in the direction of the wind in which the seas are generated.

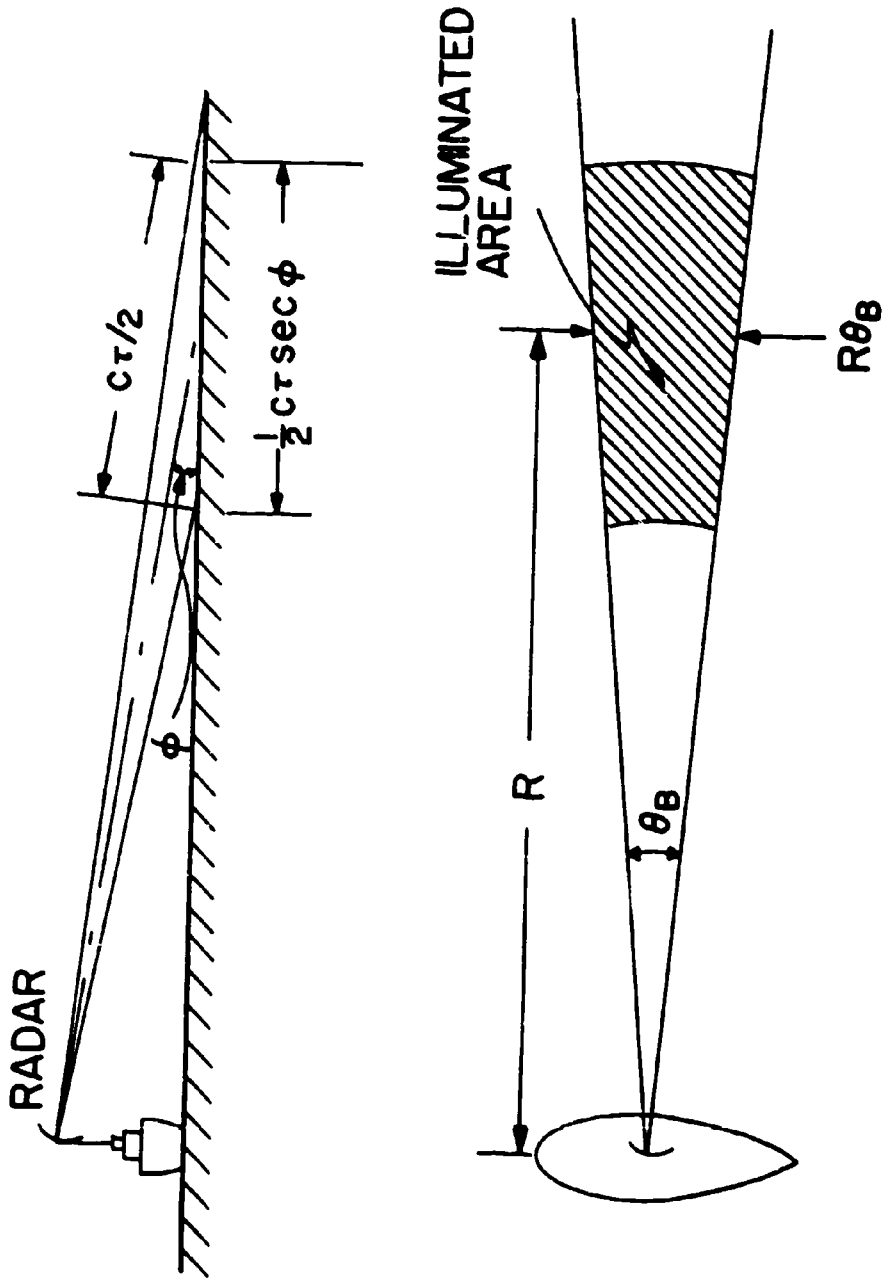


Fig. 1 - Area illuminated by radar at low grazing angles.
 (a) side view, (b) plan view. (Symbols defined in text.)

Duration -- The length of time the wind blows in essentially the same direction over the fetch.

Swell -- Ocean waves which have traveled out of their generating area. Swell characteristically exhibits a more regular and longer period and has flatter crests than waves within their fetch.

Sea -- Waves generated or sustained by winds within their fetch; opposed to swell.

Wave spectrum -- A graph showing the distribution of wave heights (or square of the wave heights) with respect to frequency in a wave record.

Sea state -- The numerical or written description of ocean surface roughness. For more precise usage, ocean sea state may be defined as the average height of the highest one-third of the waves observed in a wave train, referred to a numerical code as shown in Table 1.

Fully-developed sea (also called fully-arisen sea) -- The maximum height to which ocean waves can be generated by a given wind force blowing over sufficient fetch, regardless of duration, as a result of all possible wave components in the spectrum being present with their maximum amount of spectral energy.

Significant wave height -- The average height of the or. third highest waves of a given wave group. (Height is the vertical distance between a crest and a trough.)

There have been three qualitative scales to describe sea state, Table 1. The Hydrographic Office, or Douglas scale, has been widely used but it is supposed to be replaced by the World Meteorological Organization (WMO) Code 75¹ shown in the right hand column. The Douglas scale in its complete form (not shown in the table) specifies two numbers, one to describe the sea and the other the swell. A third system is the Beaufort number for reporting wind speeds, which dates back to the early nineteenth century. The Beaufort number, in addition to specifying the wind speed, sometimes has been used to describe the corresponding effect on the sea since there is a correlation between the wind and the sea conditions. Any qualitative description of the sea is not as meaningful to the radar designer as specifying the value of σ^0 that corresponds to the sea conditions. In many instances of radar design, the sea state number

Table 1*

**BEAUFORT SCALE
WITH CORRESPONDING SEA STATE CODES**

Beaufort number	Wind speed			Seaman's term	W.M. Measure Applied Official Code (1946)	Estimating wind speed		Hydrographic Office		World Meteorological Organization	
	knots	mph	meters per second			Effects observed at sea	Effects observed on land	Terms and heights of waves, in feet	Code	Terms and heights of waves, in feet	Code
0	under 1	under 1	0.0-0.2	Calm	Calm	Sea like mirror.	Sea like mirror.	Calm, smooth seas vertically.	Calm, 0	Calm, glassy, 0	0
1	1-3	1-3	0.3-1.5	Light air	Light air	Ripples with appearance of scales; no foam crests.	Ripples with appearance of scales; no foam crests.	Small drift indicates wind direction; waves do not mark.	Smooth, less than 1	Calm, glassy, 0	0
2	4-6	4-7	1.6-3.3	Light breeze	Light breeze	Small waves; crests of glassy appearance and breaking.	Small waves; crests of glassy appearance and breaking.	Wind felt on face; leaves rustle; waves begin to mark.	Slight, 1-3	Calm, 1/4	1
3	7-10	8-12	3.4-5.1	Overcast breeze	Overcast breeze	Large waves; crests begin to break; spray is visible.	Large waves; crests begin to break; spray is visible.	Leaves rustle (1/2) in constant direction; light flag extended.	Moderate, 3-5	Light, 1/4-1/2	2
4	11-16	13-18	5.7-7.9	Moderate breeze	Moderate breeze	Small waves, becoming longer; numerous whitecaps.	Small waves, becoming longer; numerous whitecaps.	Dist. leaves and loose paper raised up; small branches move.		Slight, 3-4	3
5	17-21	19-24	8.0-10.7	Fresh breeze	Fresh breeze	Moderate waves, taking longer form; many whitecaps; some spray.	Moderate waves, taking longer form; many whitecaps; some spray.	Small trees in leaf begin to sway.	Rough, 5-6	Moderate, 4-6	4
6	22-27	25-31	10.8-13.8	Strong breeze	Strong breeze	Larger waves forming; whitecaps everywhere; much spray.	Larger waves forming; whitecaps everywhere; much spray.	Large branches of trees in motion; whistling heard in wind.		Rough, 8-13	5
7	28-33	32-39	13.9-17.1	Moderate gale	Moderate gale	Sea heave up; white foam from breaking waves begins to be blown in streaks.	Sea heave up; white foam from breaking waves begins to be blown in streaks.	Whole trees in motion; resistance felt in walking against wind.	Very rough, 9-12		6
8	34-40	39-46	17.2-20.7	Fresh gale	Fresh gale	Moderately high waves of greater length; edges of crests begin to break irregularly; foam is blown in well-ventilated spray.	Moderately high waves of greater length; edges of crests begin to break irregularly; foam is blown in well-ventilated spray.	Trunks and small branches broken off trees; prostrate generally uprooted.		Very rough, 13-20	7
9	41-47	47-54	20.8-24.6	Strong gale	Strong gale	High waves; sea begins to roll; foam visible.	High waves; sea begins to roll; foam visible.	Slight structural damage occurs; ships heave from sea.	High, 15-20		8
10	48-55	54-62	24.5-28.4	Whole gale	Whole gale	Very high waves with overhanging crests; foam is blown in very dense streaks; rolling is heavy and violent.	Very high waves with overhanging crests; foam is blown in very dense streaks; rolling is heavy and violent.	Slight damage to land; trees broken off; considerable structural damage occurs.	Very high, 20-25		9
11	56-63	64-72	28.5-32.6	Revere	Revere	Exceptionally high waves; sea covered with white foam; pitching; visibility still more reduced.	Exceptionally high waves; sea covered with white foam; pitching; visibility still more reduced.	Very heavy experienced on land; damage usually accompanied by widespread damage.	Moderate to high	Very high, 25-30	10
12	64-71	73-80	32.7-36.9								
13	72-80	80-90	37.0-41.4								
14	81-90	90-100	41.5-46.1								
15	91-100	100-114	46.3-51.9								
16	101-109	114-128	51.9-58.9								
17	110-116	129-146	58.1-67.3								

Note: Also January 1, 1954, weather map symbols have been based upon wind speed in knots, at 80-knot intervals, rather than upon Beaufort number.

*From Revditch, "American Practical Navigator", U.S. Navy Hydrographic Office H.O. Pub. No. 9, 1966, Appendix B.

is too fine a scale considering all the uncertainties associated with its measurement and its relation to σ^0 so that a courser description is often employed; such as, for example, dividing the sea into the three regimes of smooth, medium, and rough.

Kinsman³ gives the following estimate of the percentage occurrence of wave heights for the ocean as a whole:

wave height (ft)	0-3	3-4	4-7	7-12	12-20	over 20
frequency of occurrence (percent)	20	25	20	15	10	10

Thus 45 percent of the ocean waves are less than 4 feet high, 80 percent are less than 12 feet high, and only 10 percent are greater than 20 feet high. The relative frequency of wave heights in the various regions of the world may be found in Ref. 3.

Sea waves are generated by the wind and differ from swell in both physical appearance and in their effect on radar echo. Individual sea waves are more peaked than pure sine waves and tend to be skewed in the direction of propagation. They are irregular, chaotic, short-crested (length along the crest of the same order of magnitude as the wavelength), mountainous and unpredictable except in a statistical sense. Sea waves contain many small waves superimposed on the larger waves and their spectrum covers a wide range of frequencies and directions. Swell waves are more regular than sea waves, are longer crested, have more rounded tops and are more predictable. Their spectrum covers a narrow range of frequencies and directions. Periods range from 5 to 30 sec. Swell waves in the absence of wind return considerably less radar echo than sea waves.

Gravity-wave characteristics are controlled by gravity. Both wind-generated sea waves and swell can be included in this category. The period of gravity waves varies from about one sec to 30 sec. In deep water (depth greater than a half a wavelength), classical wave theory gives the following approximate relations for the wavelength L (ft), the period T (sec) and the velocity v (knots):⁴

$$L = 5T^2$$

(1)

$$v = 3T$$

(2)

These apply to individual sine waves and it should be cautioned that they might not correctly describe measurements of the average parameters of an irregular sea.

Capillary waves have periods less than about 0.1 sec. Like sea waves they are generated by the wind but surface tension rather than gravity is the force controlling their characteristics. Wavelengths less than about one inch are considered capillary waves. Waves of longer period and length for which surface tension cannot be neglected are classed as ultra-gravity waves. Capillary waves are quite sensitive to the wind. If the breeze that generated the capillary waves dies out, they soon flatten and the sea abruptly becomes smooth again. This is in contrast to gravity waves. If the wind generating gravity waves stops, they continue to run and become swell. The phase velocity of capillary waves decreases with increasing wave height, exactly opposite to the way gravity waves behave. When capillary waves interact with the longer gravity waves, the capillary waves appear to be concentrated, at times, on the forward face of the gravity wave just before the sharp crest.^{44, 50} The crests of short capillary waves are found to be almost parallel to the wind in some experiments.⁵⁰ The crests of capillary waves are generally long and rounded with short sharp troughs.² Capillary waves seem to be the dominant scatterer when the sea is viewed by radars at the higher microwave frequencies (X band or greater).

The wave height is not fixed in relation to the wavelength, but depends on the wind generating it. Theoretical considerations show that a wave becomes unstable and breaks if the angle formed by the crest approaches 120° and that the height can be no greater than $1/7$ of the length. Observations of gravity waves indicate the height-to-length ratio to vary from 0.1 to 0.008.² The ratios for capillary waves can be greater. From the analysis of Crapper as reported by Kinsman² the maximum height-to-length is 0.73 for capillary waves controlled by surface tension. They do not break as do gravity waves, but entrap air in the troughs beyond the maximum height-to-length ratio.

It takes a finite time for a sea to develop once the wind is blowing. The term fully developed sea describes the condition when the ocean waves have reached their maximum height when generated by a given wind force. Figure 2 shows the average wave height, the significant wave height and the average height of the one-tenth highest waves as a function of wind speed when the sea is fully developed. A wind velocity of 10 knots blowing for 2.4 hours over a fetch of at least 10 nm produces a fully developed sea with a significant wave height of 1.39 ft.¹¹ A 20 knot wind over a 75 nm fetch blowing for 10 hours results in a fully developed sea with a significant wave height of 7.9 ft. A 30 knot wind and 23 hour duration give a height of 21.7 ft if the fetch is 280 nm. Figure 3 shows the growth of wave height with wind duration for a wind speed of 20 knots.

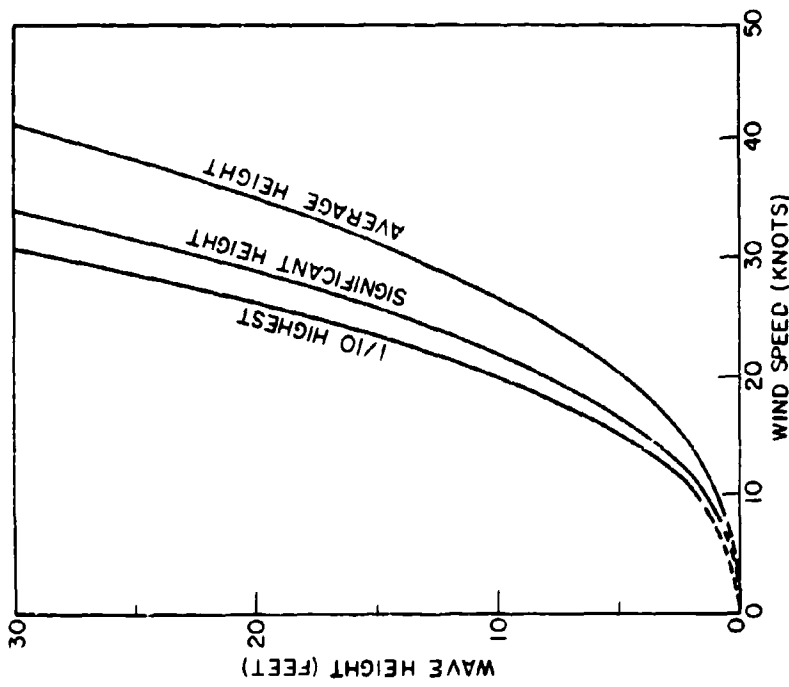


Fig. 2 - Wave height of the fully developed sea as a function of wind speed. Significant height = 1.6 x average height, 1/10 highest = 2.04 x average height. (Adopted from H.O. Pub. No. 603. ¹¹)

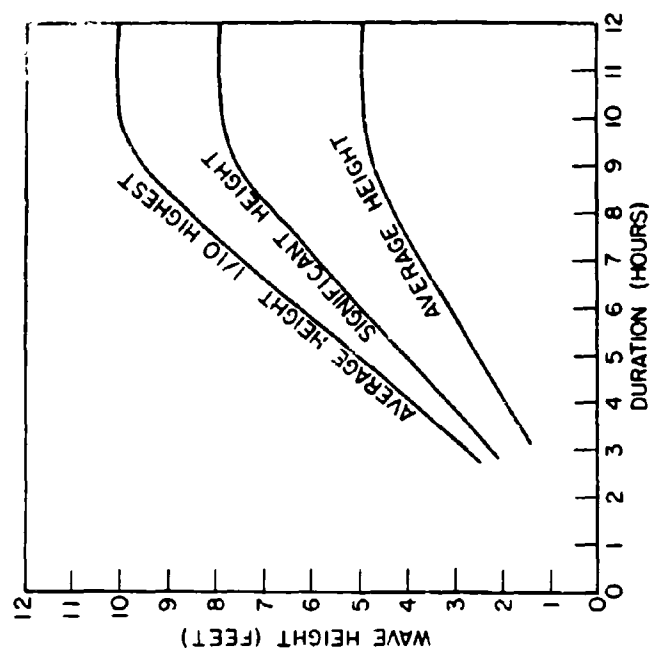


Fig. 3 - Build up of wave height with time for a constant wind speed of 20 knots and a fetch greater than 75 naut mi. (Adapted from H.O. Pub. No. 603. ¹¹)

If the height of the water surface were recorded at some point, the variation of height with time would not be a simple sinusoid but, in general, it would appear noise-like. Being noise-like means that the precise variation of height with time cannot be predicted from the preceding measurements anymore than can the voltage waveform of receiver noise be predicted precisely on the basis of past measurements. A record of the wave height at a particular location would also bear little resemblance to the waveform at some other location. Thus the height of the sea surface is found to be random with time and location with a distribution that can be approximated by a Gaussian statistical process.⁴⁶

Although the statistical nature of the sea surface was recognized in the early days of wave research, the complexities of statistical analysis were avoided by assigning average values to wave lengths, periods, directions and other wave properties. Average values are convenient to use and simplify the discussion of wave properties but they are not suitable descriptors of the sea for many purposes and the statistical characterization of the sea must be introduced. The usual method for expressing statistical wave properties is by the power spectrum. This is a plot of the distribution of the square of the wave heights as a function of the wave frequency (or wavelength) and the direction. The wave spectrum is thus a function of the two parameters of direction and wave frequency and can be pictured as a two-dimensional contour plot with frequency and direction as coordinates.⁴⁸ Figure 4 is a representation of such a two-dimension contour plot. (The contours are of dimension $\text{ft}^2\text{-sec.}$) Oceanographers generally give the wave spectrum in terms of the square of the wave height rather than the wave height since the average energy per unit area of the sea surface is $g \rho \overline{h^2}$, where g = acceleration of gravity, ρ = density of water, and $\overline{h^2}$ is the mean square elevation (or depression) of the sea surface from the undisturbed sea level.⁴⁷

Two dimensional wave spectra are difficult to measure and a one-dimensional spectrum is often used by integrating the effects of direction. Figure 5 is an example of a one-dimensional wave spectrum for several wind speeds. Note that the displacement of the maximum spectral energy decreases to lower frequencies (longer wavelengths) with increasing wind speed.

Measured spectra generally apply to the longer gravity waves because of the difficulty of observing the small capillary waves in the presence of the larger waves. The frequency transition between capillary and gravity waves is sometimes taken as 13.5 Hz. This is the wave frequency at which the phase velocity is a minimum. It corresponds to a wavelength of 1.7 cm and a velocity of 23 cm/sec. At both higher frequencies (capillaries) and lower frequencies (gravity waves) the phase

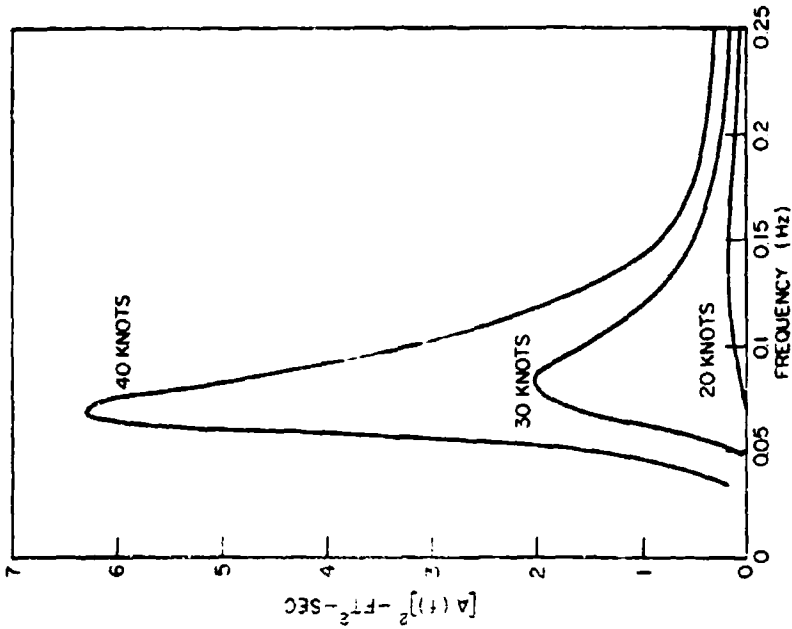


Fig. 5 - Approximate wave spectra for winds from 20 to 40 knots. (Adapted from Refs 11 and 49.)

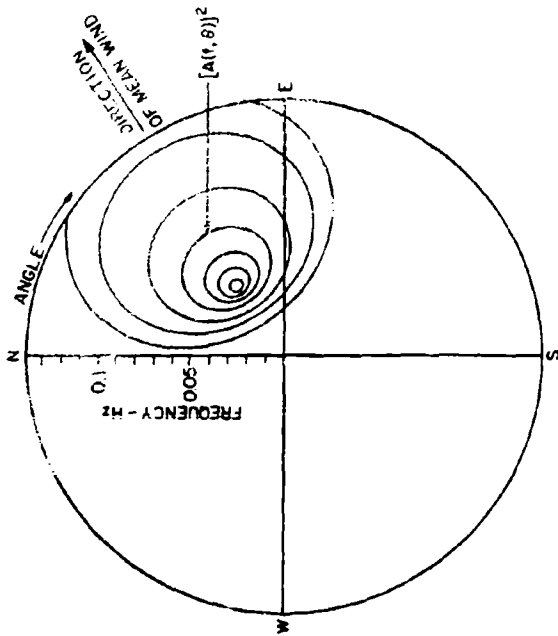


Fig. 4 - Approximate representation of a two-dimensional wave spectrum in polar coordinates (frequency, angle). Contours of constant $[A(f, \theta)]^2$ increase toward center.

velocity is higher.⁵⁰ From laboratory measurements of capillary wave spectra there is a tendency for the spectrum to peak at high frequency. The peak moves to higher frequencies and broadens with increase in wind speed. The cutoff at still higher frequencies results from the inability of the wind to supply energy to shorter waves at a sufficiently rapid rate to overcome viscosity.⁵⁰

2. GRAZING ANGLE

Figure 6 depicts how σ^0 might vary as a function of the grazing angle.* Three distinct regions can be identified. In the quasi-specular region near vertical incidence the radar echo is quite large. Measured values of σ^0 at 90° often lie between 0 db and +10 db for medium seas. (It is common to express σ^0 in decibel notation, that is, $\sigma^0(\text{db}) = 10 \log_{10} \sigma^0$.) The large echo at vertical incidence is called the altitude return and is apparently due to specular scatter from facet-like surfaces oriented in the direction of the radar. Altitude return is of importance in designing radars that operate over water since the echo at vertical incidence sometimes can be large enough to allow energy to enter the radar via the sidelobes and interfere even when the main beam is pointing at some angle at which the sea echo is low.

Water waves cannot achieve too large a slope without breaking and becoming spray and droplets. Thus, below some grazing angle there will be little likelihood of significant specular return from the facets constituting the surface of the sea. In the preceding section it was noted that the maximum included angle at the crest could be no less than 120° , which would make the minimum grazing angle for quasi-specular reflection to be 60° . The plateau region is the name given to that part of Fig. 6 where the grazing angles are below those which produce quasi-specular reflection from facets. Sometimes this is called the diffuse region. The boundary between the plateau region and the quasi-specular region is called the transition angle. The transition is a gradual one and it is difficult to define a precise boundary. (Sometimes the transition angle appears more evident when the angle coordinate (abscissa) is plotted on a logarithmic

*The term grazing angle is more commonly used than incidence angle. The former is measured from the horizontal, the latter from the vertical. The depression angle is also measured from the horizontal, but at the radar antenna rather than where the radar beam intersects the surface. When the earth's curvature must be considered, the depression angle and the grazing angle are not equal as they would be for a "flat" earth.

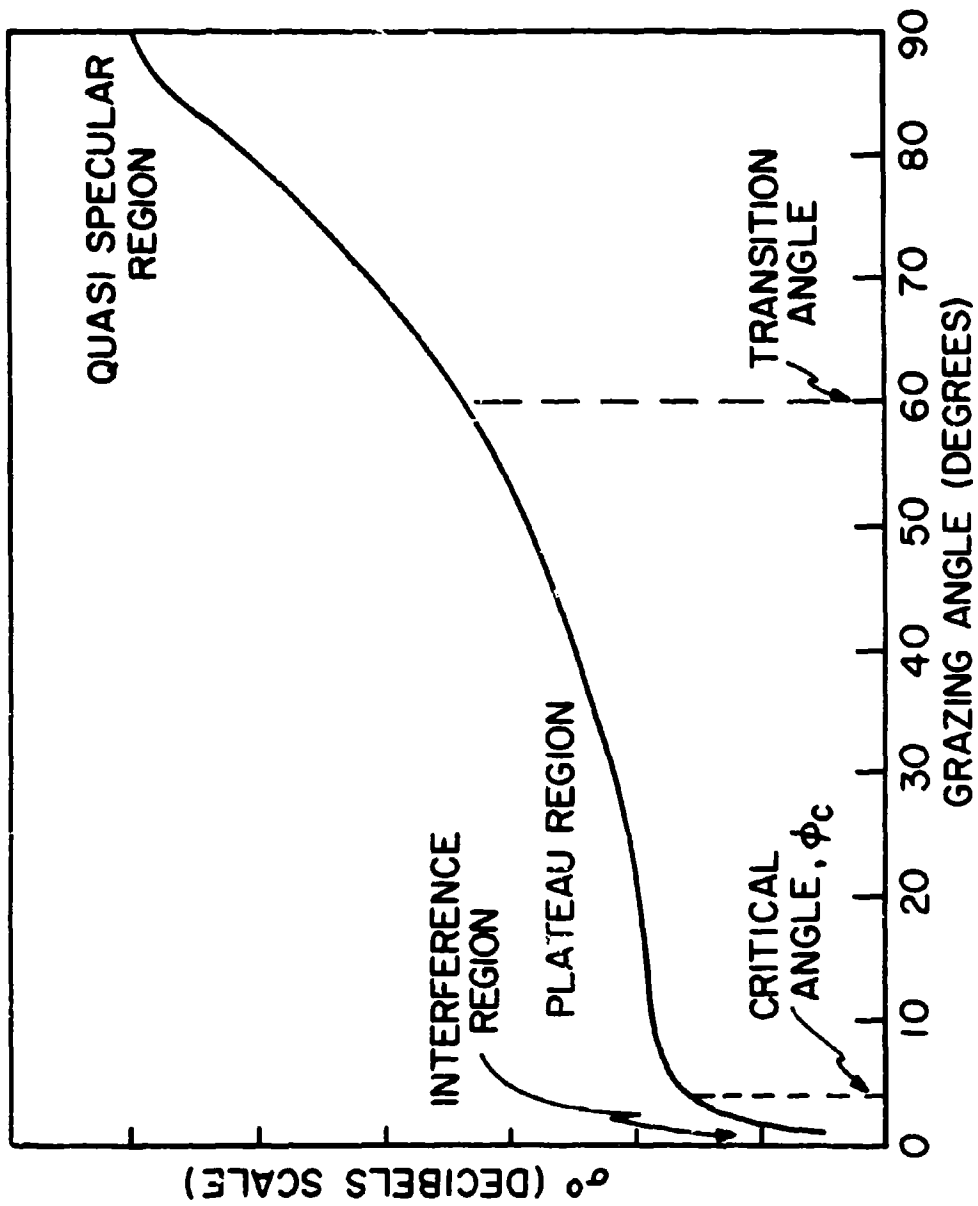


Fig. 6 - Representative example of the variation of σ^0 with grazing angle

rather than a linear scale. It is also more evident with measurements made of a calm sea rather than one that is rough.) The value of σ^0 in the plateau region for vertical polarization decreases slightly with decreasing angle; some experiments show a decrease of about 0.15 db/degree at microwave frequencies. With horizontal polarization, the slope of the σ^0 curve seems to be greater the lower the frequency. Backscatter from the sea in the plateau region is similar to backscatter from a rough surface. The chief scatterers in this region are those elements of the sea that are of dimension comparable to an RF wavelength and which ride on top of the larger-wave structure.

At very low grazing angles, of the order of several degrees or less for microwave frequencies, σ^0 decreases rapidly with decreasing angle. In this region the direct wave interferes with the wave reflected from the surface in a manner similar to that experienced for propagation over a smooth earth, hence the name interference region. The approximate angle at which transition occurs between the plateau and interference regions is called the critical angle. The critical angle is generally easier to identify experimentally than the transition angle. With sufficiently low frequency the critical angle may be high enough so that neither a critical angle nor a transition angle can be readily identified. Below the critical angle, theory indicates σ^0 to vary as the fourth power of the grazing angle. The critical angle is difficult to determine precisely but it is found to depend on the frequency, polarization and sea state.⁹

The echo at low grazing angles with vertical polarization is also affected by the Brewster angle.* At the Brewster angle the reflection coefficient is a minimum and the forward scattered wave is small and interference effects are less prominent. Also at low angles, shadowing of the area behind the waves can modify the nature of the echo for either polarization.

Measurements of σ^0 as a function of angle have been carried out in at least three different ways. The most convenient is from land looking over the water. Grazing angles at microwave frequencies are then usually limited to less than 10° . In such experiments care must be taken to

*According to Ref. 25, this should be called a pseudo Brewster angle for the case of the sea. The classical Brewster angle is observed only for reflections from pure dielectrics. However, much of the literature on radar sea echo, including this report, fails to make this distinction.

select sites that observe sufficiently deep water so that the effect of the shore does not enter into the measurements. Suitable sites are few. Sea echo measurements have also been made from bridges overlooking water. Higher grazing angles can be obtained but bridge sites generally do not overlook water typical of ocean conditions. A third method for sea echo measurements is an aircraft-mounted radar. Higher angles of elevation can be obtained from aircraft than from a land site. Aircraft have the further advantage in that they can observe sufficiently far from land and can cover a wide region of the ocean. However, it is more difficult to know the environmental conditions and precise character of the sea from an aircraft and to make an accurate, absolute calibration of the measurement apparatus. Blimps also have been used as airborne radar platforms for sea echo measurement. Satellites offer an excellent, but expensive, means for measuring sea echo on a world-wide basis at relatively frequent observation intervals.

Figure 7 shows a composite of data derived from the results of several experiments, chiefly from those conducted over the years by the Naval Research Laboratory. It does not correspond to any particular set of experimental data but it is believed to be representative. As mentioned previously the variability of experimental sea echo data is great and does not warrant the preciseness with which Fig. 7 is apparently drawn. Even in the laboratory it is difficult to measure the absolute radar cross section to within one or two db. Greater differences are more likely when the target is of a complex nature. Under field conditions where sea echo is generally measured the degree of uncertainty can be worse than in the laboratory. It is difficult to specify the likely error in sea echo measurements, but it is the writer's opinion that agreement on a relative basis between experiments should not be expected to be better than 3 to 6 db, perhaps even worse. Thus, instead of a thin line to depict the data of Fig. 7, a broad strip perhaps ± 3 db in width might be drawn to indicate uncertainty. (This was not done in this figure since it would have resulted in a confused drawing because of the overlap among the bands ± 3 db in width.) Even though the individual data from which this set of curves was drawn was highly variable, the composite is believed to be more reliable than any of its parts because of the "smoothing" that can be accomplished when plotting the data available over a range of frequencies and other experimental conditions. Figure 7 was derived from a variety of data extending over a range of wind speeds of roughly 10 to 20 knots. Although this is a relatively broad range of wind and sea state, the variability of the available data does not permit narrower limiting of these parameters at the time of writing. The radar system designer must recognize the variable nature of sea echo and take proper account of its variation during design.

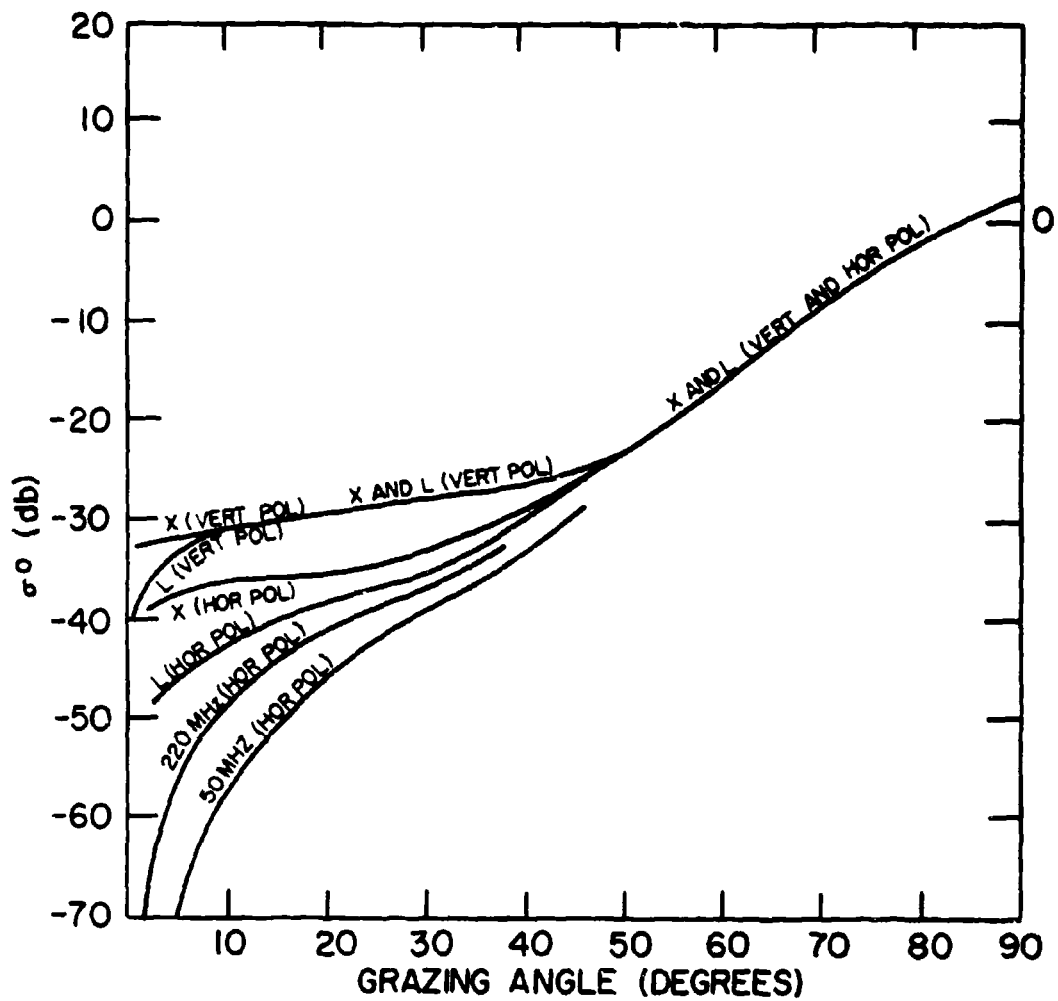


Fig. 7 - Composite of data showing the variation of σ^0 with grazing angle, frequency and polarization for a "medium" sea.

According to Fig. 2 and Table 1, the sea state ranges from 2 to 4 for winds ranging from about 10 to 20 knots. Thus Fig. 7 data might be described as a medium sea and might correspond to a state 3 sea. Figure 7 also indicates the frequency and polarization dependence. The data for 220 MHz²² extended only to 14° but was (boldly) extrapolated to higher angles. The experimental data for 50 MHz²³ did not extend to low angles; but since this is in the interference region, the curve was extrapolated according to a θ^4 law. Both the 220 MHz and the 50 MHz data were taken at a lower sea state than the higher frequency data. The data is included here nonetheless since no other was available and since it is guessed that the difference between sea state 1 and sea state 3 is hopefully small at these frequencies and grazing angles.

Above about 10°, σ^0 for vertical polarization appears the same at both X and L bands. There is some indication that the sea echo with vertically polarized radiation is independent of frequency in the plateau region and the quasi-specular region if the frequency is below X band.¹⁹ Above X band the vertically polarized echo seems to increase with frequency as indicated by the data of Grant and Yaplee⁹ shown later in Fig. 8. In the quasi-specular region, sea echo appears independent of both the frequency (at least at X band and below) and the polarization.

3. SEA STATE AND WIND

It is difficult to measure experimentally the effect of the wind and sea state on radar echo. Such measurements require a substantial period of time to obtain a wide variation of sea and wind conditions. Since the sea state depends on the wind it is not always easy to determine which is the more important factor affecting the radar echo from the sea. Generally at the higher microwave frequencies (X band or above) and low grazing angles, the wind is found to be a significant parameter with which to correlate radar sea echo. At the lower frequencies and higher grazing angles the wave characteristics are probably more significant than the wind velocity.

If the sea is calm and undisturbed by the wind, the radar echo is small (except at angles near normal incidence). As the wind builds up and exceeds approximately 5 to 10 knots, the sea echo increases rapidly from its very small value. It takes a finite time for the waves to build up as was shown in Fig. 3. The greater the wind the longer it takes for the sea to become fully developed. It is common to observe old wind waves, present wind waves and swells existing at the same time. The fact that swells often arrive in an area from a direction other than the local wind also contributes to the variability of data.

Capillary and short gravity waves are excited in a matter of seconds and the radar backscatter at the higher microwave frequencies builds up quickly with the wind. At the lower frequencies, the increase in sea echo lags in time the build up of the wind because of the duration required for development of the longer water waves. There is much experimental evidence to show that in the absence of wind there is but a small sea echo at the higher microwave frequencies. Swell with waves as high as 10 ft have yielded but low sea echo when viewed at low grazing angles with X band in the absence of wind.

From the observations of sea echo with wind it appears that the X-band echo is associated with capillary waves. These are of a wavelength comparable to the radar wavelength. Another important piece of experimental evidence relating the X-band sea echo to capillary waves is that when contaminants, such as oil, are introduced in the water the capillary waves are dampened and the microwave sea echo is reduced. Controlled laboratory experiments in water tanks also show the importance of capillary waves at microwave frequencies.¹²

In spite of the difficulties of describing the sea conditions and winds, the effect of these factors on sea echo has been studied and some general trends can be discerned. Generally, σ^0 will increase as the sea becomes rougher except at angles near vertical incidence where the opposite effect occurs.

Grant and Yaplee⁹, using a bridge-mounted radar overlooking a river, made observations of the sea echo as a function of wind at wavelengths of 8.6 mm, 1.25 cm and 3.2 cm (Fig. 8). They indicated, and many others have verified, that for wind velocities below 5 knots the echo was quite small, except at grazing angles near the perpendicular. For glassy calm water the reflection at normal incidence was very high (theoretically σ^0 is equal to $G/4$, where G = gain of the observing antenna, when viewing a perfect reflector at normal incidence) and decreased more than 35 db at angles only 10° from normal incidence. They found that for grazing angles near 90° (normal incidence), σ^0 was reduced by the presence of the wind. At grazing angles less than about 80° , σ^0 increased in the presence of wind.

Measurements by Macdonald¹⁰ at L band show similar effects of the wind, Fig. 9. As the grazing angle varies from 50° to 8° the value of σ^0 decreases from -30 to -60 db for horizontal polarization and low winds. This data also shows that σ^0 is more sensitive to wind when the polarization is horizontal rather than vertical.

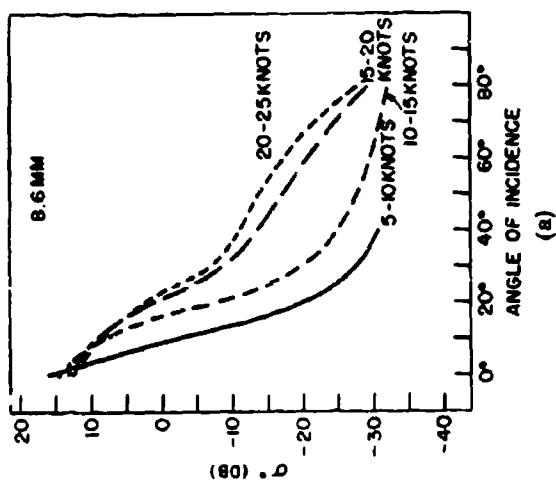
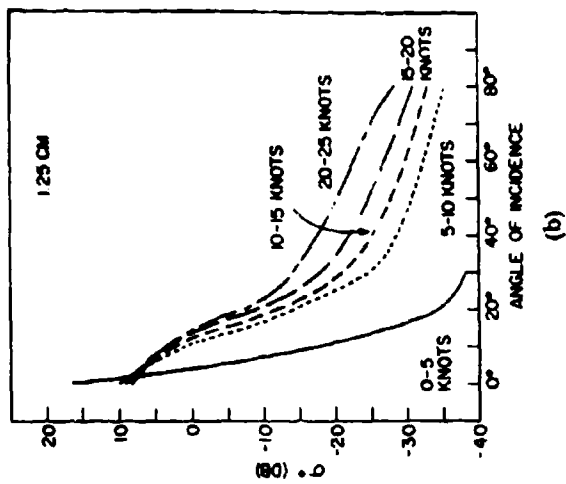
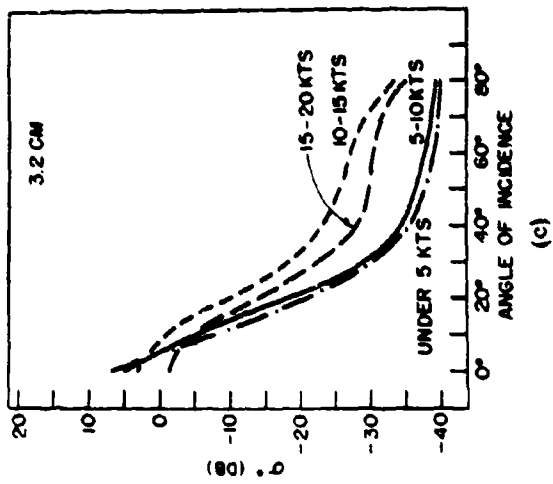


Fig. 8 - σ° as a function of grazing angle and wind speed for vertical polarization. (a) $\lambda = 8.6$ mm, (b) $\lambda = 1.25$ cm, (c) $\lambda = 3.2$ cm. (From Grant and Yaplee. ⁹)

Experimental measurements made at X band at low grazing angles show σ° to increase rapidly with wave height but indicate little or no increase when the wave height is greater than about 2 to 3 ft.¹³

The variation of σ° with angle in the vicinity of normal incidence seems to be related to the distribution of the water wave slopes which in turn depends upon the sea state or roughness. Figure 10 illustrates the nature of this theoretical dependence. These curves are computed for various values of the rms slope of the sea surface, $\tan \beta_0$, and apply to the higher microwave frequencies. As the surface becomes rougher β_0 increases and the echo at normal incidence is less. This variation with β_0 might be used to determine the surface roughness by radar measurements of σ° as a function of angle in the quasi-specular region. The radar might be located in an aircraft or a satellite.

Figure 10 is based on the analysis of Spizzichino⁸ who considered the surface of the sea to consist of elemental "mirrors," or facets, much larger than the RF wavelength. The major part of the scattering is due to those facets oriented in the direction of the radar. If the facets are distributed normally with an rms slope $\tan \beta_0$, the sea clutter coefficient is

$$\sigma^{\circ}(\theta) = \mu \cot^2 \beta_0 \exp\left(-\frac{\cot^2 \varphi}{\tan^2 \beta_0}\right) \quad (3)$$

where φ is the grazing angle. The value of μ is said to be of the order of unity at X band and in the millimeter wave region.⁸ It also seems to be independent of the sea state and the wind speed at these shorter wavelengths. At UHF, μ appears to be much smaller and might be about 0.1, but the data on which this is based is limited. (These values of μ are based on experimental data. It would seem, however, that μ should at least equal the reflection coefficient.) At $\varphi = 90^{\circ}$ and when $\mu = 1$, Eq. (3) shows $\sigma^{\circ} = \cot^2 \beta_0$. Thus σ° at normal incidence is the inverse square of the rms slope of the surface. Although this model gives results in rough qualitative agreement with experiment, measurements differ significantly from this theory in both the value at normal incidence and the rate of decrease with decreasing angle. The theoretical curves of Fig. 10 do not seem to fall off as rapidly as shown by experiment and the crossover at which σ° increases with wind instead of decreases is about 50 to 70° instead of the observed 80 to 85° . Thus Eq. (3) and the theory on which it is based should be suspect.

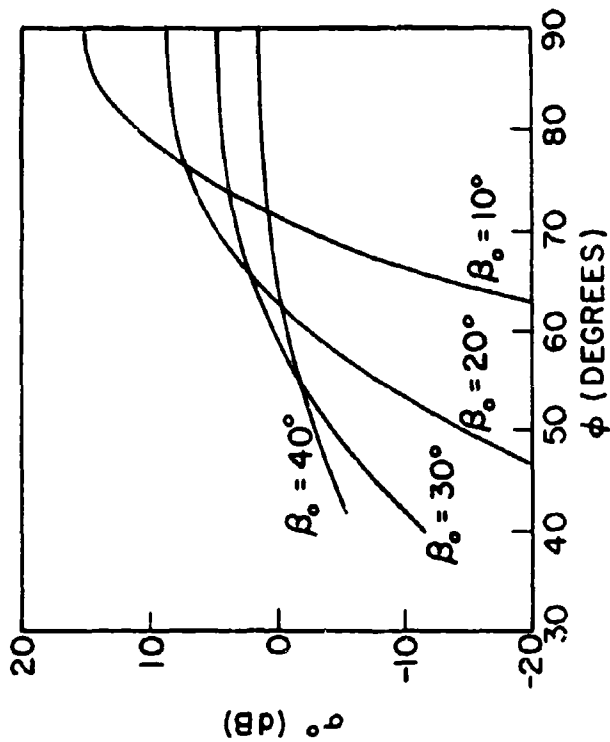


Fig. 10 - Theoretical variation of σ^0 versus grazing angle based on a model of the sea surface consisting of randomly distributed facets governed by a Gaussian law with an rms surface slope = $\tan \beta_0$. (After Spizzichino. ⁶)

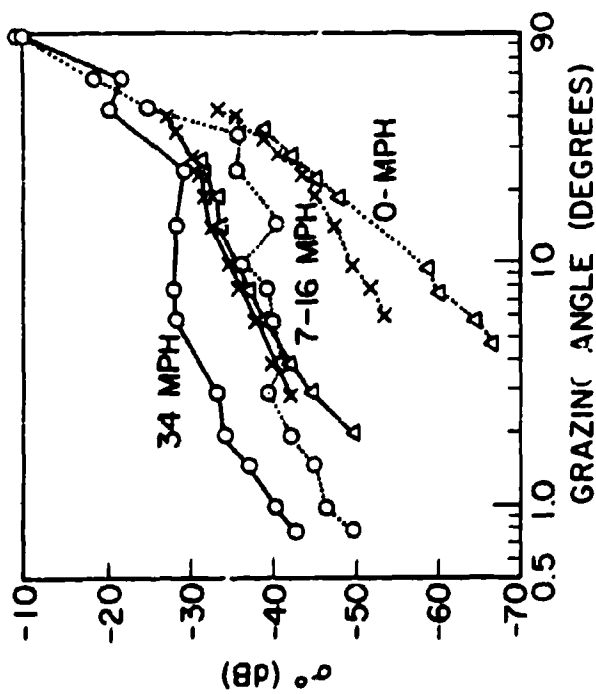


Fig. 9 - σ^0 as a function of grazing angle and wind speed, 1250 MHz. Solid line -- vertical polarization. Dotted line -- horizontal polarization. (From MacDonald. ¹⁰)

The effect of wind depends on the grazing angle. At normal incidence, σ° decreases with increasing wind as shown in Fig. 11. This is a composite of data at X band and L band. The two are drawn on the same curve assuming there is negligible frequency dependence of σ° at normal incidence. At normal incidence the usual meaning of "horizontal" and "vertical" polarization disappears.

In the plateau region the opposite occurs in that σ° increases with increasing wind. From about 5 to 30 knots the microwave radar echo increases with increasing wind at the rate of about 0.8 db/knot when the polarization is horizontal and the grazing angle is approximately 10° . The increase with vertical polarization is less but the data is too uncertain to state how much less. For want of a better number some data indicates a variation of about 1/3 db/knot. In the vicinity of 60° grazing angle the sea echo increases at about 1/3 db/knot with horizontal polarization. At winds from 30 to 40 knots σ° increases at a slower rate, perhaps 0.2 to 0.3 db/knot or less in the plateau region (10° grazing angle). Some observers report a saturation at higher wind speeds where no increase in σ° is found with increasing wind.^{7, 29} One of the difficulties in relating experimental σ° data to the reported wind speeds is that it is seldom reported when the sea is fully developed so that the wind might not always be a true indicator of sea conditions.

Wu⁴³ has shown that the interaction of the wind on the water can be divided into three regimes. At very low wind velocity (a "breeze" less than 3 m/sec, or about 6 knots) the air flow near the surface is aerodynamically smooth. This corresponds to sea state 0 to 1 and Beaufort number 0 to 1. For winds between 3 m/sec and 15 m/sec (6 knots and 30 knots, sea state 1 to 4, or Beaufort number 1 to 6) the surface roughness increases with wind until it reaches a saturation at 15 m/sec, or 30 knots. Above 15 m/sec the wind velocity is greater than the average wave phase velocity. As the wind blows harder, the transfer of more energy from the air merely provides energy to waves with large wavelengths. The very high phase velocities and relatively flat shapes of these waves do not contribute to surface roughness.¹¹ Wu suggests that the surface roughness is governed by the amplitude of the short gravity waves rather than the mean square surface slope. These three regimes seem to agree qualitatively with microwave radar observations of sea echo. In the aerodynamically smooth region (less than 3 m/sec) the sea echo is found to be small. The sea echo increases with increasing wind when the surface roughness increases with wind speed from 3 m/sec to 15 m/sec. The presence of a saturated condition with winds greater than 15 m/sec, or 30 knots, is also consistent with radar experience.

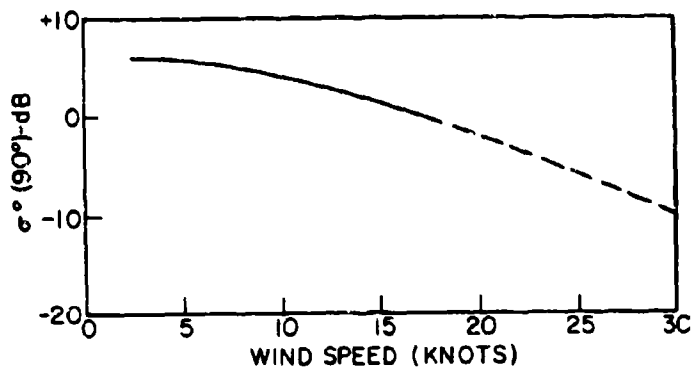


Fig. 11 - σ^0 as a function of wind for normal incidence ($\phi = 90^\circ$). Solid curve is based on the data of Grant and Yaplee⁹ at X band. Dashed curve is an extension to include the L-band data of Macdonald¹⁰ at 30 knots wind speed.

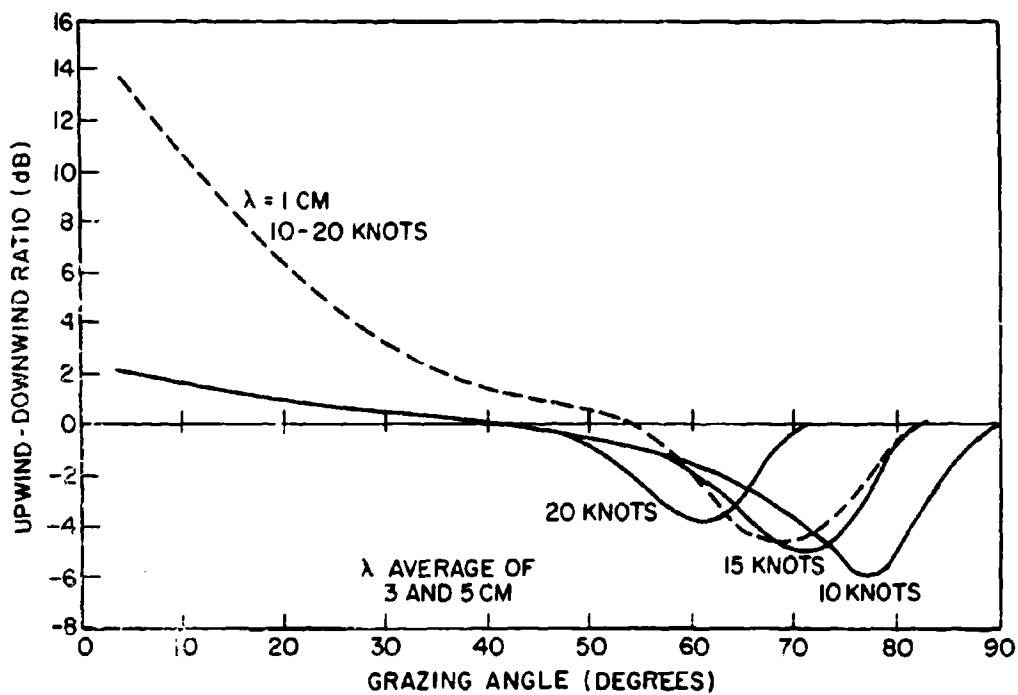


Fig. 12 - Upwind-downwind ratio of radar return from a wind-swept water surface as a function of grazing angle for three wind velocities for $\lambda = \text{avg. of 3 and 5 cm}$ data derived from water wave tank measurements. Dashed curve is for $\lambda = 1 \text{ cm}$.¹⁴

Many observers have noted that the upwind sea echo (radar looking into the wind) is generally greater than the values obtained from other viewing aspects. Schooley¹⁴ has measured the statistical distributions of facet size (facets are the small patches of the sea surface assumed in some models of the sea to be the elemental scatterers), in relationship to wind velocity, facet slope and flatness tolerance (defined as one-tenth the radar wavelength). These measurements were made in a wind tunnel with water as a lower surface. Although the fetch available in a tank is short and the conditions in a tank may not be as in the ocean, the results are not too inconsistent with the wide spread of experimental data. Figure 12 illustrates computed results as derived from the water wave tank measurements. At low grazing angles the radar return from a wind-swept water surface is greater when the radar is pointing into the wind than when it is pointing at the same angle downwind. This is more pronounced at the higher frequencies than at the lower frequencies. In the grazing angle region between approximately 50° and 80° the radar returns are greater when looking downwind than when looking upwind at the same angle. According to Schooley this is probably due to the specular reflections off the broad gentle slopes of the waves. Schooley's measurements of flatness tolerance limited his theoretical analysis to frequencies no lower than S band (10 cm wavelength). No polarization dependence was included. Marks⁴¹ using stereoscopic camera data on facet size distribution of 1 to 1.5 foot high ocean waves has obtained better agreement with actual radar measurements of upwind-downwind ratio than the data obtained by Schooley in a model wave tank. Figure 13 shows experimental data of the upwind-downwind and upwind-crosswind ratios.

It is important to note that the ocean currents relative to the direction of the wind can affect measurements of σ^0 . For example, it has been observed that the echo obtained from the Gulf Stream off the coast of Florida is appreciably larger when the direction of the wind is from the north or northeast than if the same wind speed is observed from the south or southeast. Since the Gulf Stream flows to the north, when the wind is from the north against the Gulf Stream its speed adds to that of the water v_g and the air-to-sea relative velocity is increased by v_g . Likewise, if the wind is with the stream, its speed v_g subtracts so there is a difference of $2 v_g$ in the relative speed depending on the direction of the wind with respect to the current. It seems evident that due to this difference of $2 v_g$, the energy that a given wind delivers to the ocean is greatly increased near the continental United States if the wind is from the north or northeast (against the Gulf Stream). This could be one reason why differences have occurred in measurements since very few, if any, radar observers have included values of ocean currents in their data.

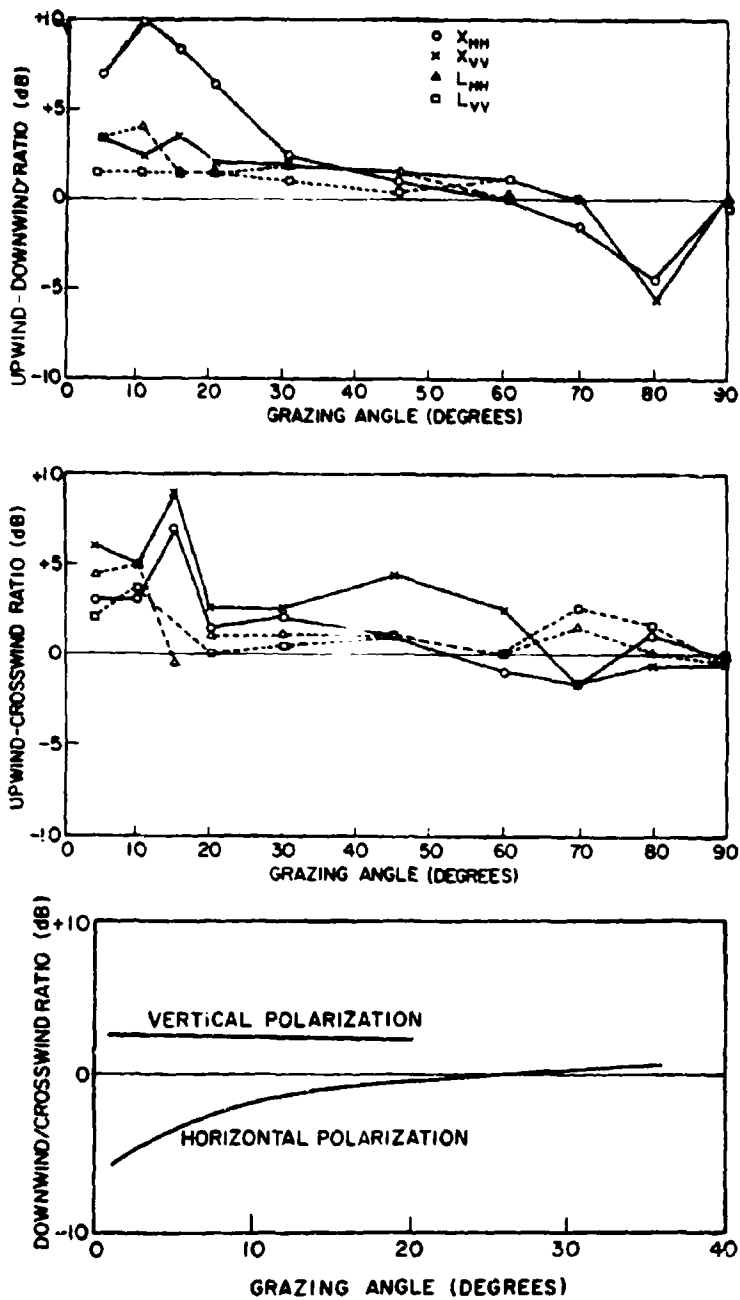


Fig. 13 - Experimental measurements of (a) upwind-downwind ratios and (b) upwind-crosswind ratios. Solid curves — X band, dashed curves -- L band. Average of six days. Median wind velocity = 10 knots. (After Ref. 32.) (c) Ratio of downwind-to-crosswind sea echo at L band. Averaged values. (From Macdonald.¹⁰)

Although most radar experiments will quote a value of the wind velocity it should be cautioned that an average value might not be too meaningful. The wind varies not only in time but in space. It may be steady or gusty. Most wind measurements are obtained at some height above the water, but the wind at the surface can be quite different. The result is that much variation can occur in data supposedly taken under similar environmental conditions as reported by individual experimenters.

The wind velocity near the air-sea interface is found to vary logarithmically with height above the surface.^{43, 44, 51} This can be expressed as

$$U_z = \frac{U_*}{k} \ln \left(\frac{z}{z_0} \right) \quad (4)$$

where U_z = mean speed at height z , U_* = friction velocity = $(\tau/\rho)^{1/2}$, τ = shearing stress, ρ = air density, k = Karman constant ≈ 0.41 and z_0 = the roughness parameter (virtual origin of the profile) which is a constant for a given uniformly roughened surface under neutral stability conditions. A standard height for wind speed measurement is 10 meters, U_{10} . The velocity at some other height relative to U_{10} is from Eq. (4).

$$U_z = U_{10} \frac{\ln(z/z_0)}{\ln(10/z_0)} \quad (5)$$

If the roughness parameter were 0.1 cm^{50} the value of U_z/U_{10} is 0.945 at 6 m (19 ft), a height often used for wind measurements. At a height of one meter the velocity is three-quarters that at 10 meters and at 6 cm it is 0.445. Care should be taken when examining experimental data to be sure the winds are measured at the same approximate height. This can be important when comparing laboratory measurements, where the wind is measured relatively close to the surface, and experimental measurements over the ocean which are often referenced to U_{10} or U_6 .

4. POLARIZATION

At grazing angles greater than about 60° from the horizontal, very little difference is noted in the sea echo for different polarizations. At low grazing angles, however, there can be significant differences, as was illustrated in Fig. 7. In calm seas with little wind, the echo obtained with horizontal polarization is considerably less than that with vertical polarization. The echo with horizontal polarization increases

with increasing wind speed faster than the increase with vertical polarization so that with rough sea conditions there is less difference in the magnitude of the echo from horizontal or vertical polarization. Some experimenters find at times the echo with X band vertically polarized radiation to be several db less than with horizontal polarization in rough seas.¹³ This has been said to occur looking crosswind along the troughs in the waves.³⁰

The ratio of the echo per unit area received on vertical polarization σ_{VV}^0 to that received on horizontal polarization σ_{HH}^0 is sometimes used to describe the effect of polarization, Fig. 14. (With this commonly used notation, the first letter of the subscript is the transmitted polarization and the second letter is that received. V = vertical polarization. H = horizontal polarization.) This ratio is seen to be less at X band (10 GHz) than at L band (1.2 GHz).

Macdonald¹⁸ makes the following observations regarding the polarization ratio: (1) It increases with wavelength. (2) It increases with decreasing sea roughness. (3) The maximum ratio can occur at angles as large as 30 degrees and return to unity ratio at grazing. (4) The angle of maximum ratio decreases with decreasing sea state.

Polarization can affect the value of the critical angle. With a simple model of the reflecting surface the critical angle is that angle below which destructive interference occurs so that the echo signal decreases rapidly with decreasing angle. The degree of destructive interference depends on the amplitude and phase of the forward propagating wave reflected by the surface relative to that of the direct wave. Since the reflection from a surface is different for the two polarizations the behavior of the echo signal at low grazing angle can also be different. On the basis of a limited amount of experimental evidence, Katzin¹⁷ gives the critical angle as

$$\sin \varphi_c = \frac{\lambda}{2h_w} \quad (6)$$

where h_w is defined by Katzin as the wave height exceeded by 10 percent of the waves and λ is the radar wavelength. (It is of interest to note that the critical angle might have been defined in other ways. A point target at a height h above a smooth surface would have a critical angle $\sin \varphi_c = \lambda/4h$. If the target were distributed uniformly over a height h , then $\sin \varphi_c = \lambda/5h$. If the Rayleigh roughness criterion were used to define the critical angle, $\sin \varphi_c = \lambda/8h$, where h is the height of the surface

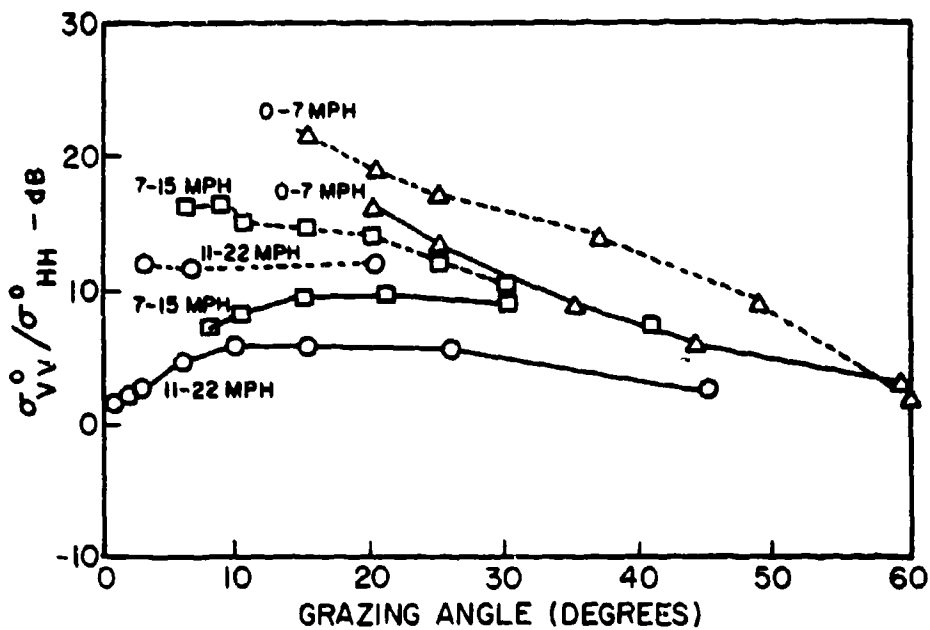


Fig. 14 - Ratio of the sea echo on vertical polarization, σ_{VV}^0 , to that on horizontal polarization, σ_{HH}^0 , for 10 GHz (solid line) and 1.2 GHz (dashed line). (From Macdonald, 1968)

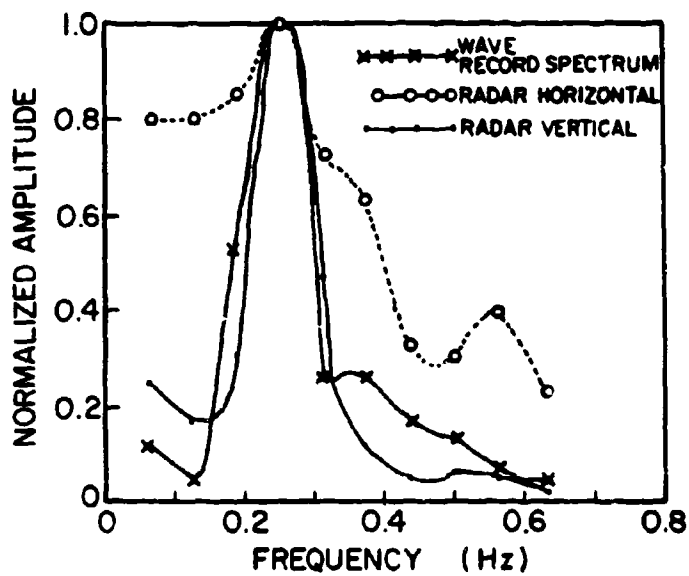


Fig. 15 - Normalized power spectra comparing water-wave record with the radar echo obtained with horizontal and vertical polarization. Data taken with X band radar, 8 nsec pulse width providing an effective illuminated area 22 ft wide by 5 ft deep. Wave height = 1.4 ft.

irregularity.) At a wind speed of 15 knots, corresponding approximately to the data of Fig. 7, the average height of the one-tenth highest waves is 5 ft. Assuming this is a good approximation of h_w , Eq. (6) predicts the critical angle to be about 0.6° at 10 GHz (X band), 4.5° at 1250 MHz (L band), 13° at 450 MHz, and 27° at 220 MHz. At 50 MHz, Eq. (6) does not give a critical angle below 90° . Since the critical angle is dependent on the wave height, it can be seen that differences in sea echo due to sea state or wind at the low grazing angles might be accounted for by the change in the critical angle brought about by the change in wave height. It must be cautioned that the critical angle as described by Eq. (6) is based on a simple model and that correlation with experiment is difficult to achieve to the "precision" implied by the example values stated in the above.

The critical angle should be more prominent with horizontal polarization since the reflection coefficient is close to unity and the phase change on reflection is approximately 180° . With vertical polarization or in a rough sea the critical angle might not always be simply expressed as in Eq. (6).

At microwave frequencies, the predominant scatterers producing sea echo are probably not the gross wave structure. Theory shows that the backscattering from a pure "sine-wave" sea would be small when viewed at angles other than those near normal incidence. Evidence seems to indicate that the scattering takes place from the individual facets or capillary waves that ride on top of the gross wave structure. An analysis of the scattering from such a target might show effects different from the simple model used to define the critical angle of Eq. (6). Furthermore, at low angles diffraction effects must be considered and the curvature of the earth might have to be taken into account. Horizontally polarized radiation does not propagate close to a conducting surface as does vertically polarized radiation. If the energy cannot propagate near the water surface there will be less reflected echo energy. This property of horizontal polarization and diffraction effects might explain why horizontally polarized L or X band radiation in Fig. 7 is less than vertically polarized radiation at low grazing angles even before the critical angle is reached. Another factor affecting the polarization behavior at low angles is the possible shadowing of one wave by another. From geometrical optics considerations, shadowing is not polarization dependent. However, it appears that geometrical optics alone might overestimate the effect of shadowing and a more exact diffraction analysis might show differences in the shadowing depending on the polarization. Still another important factor affecting the sea echo observed with the two polarizations is the Brewster angle. At the Brewster angle the reflection coefficient of vertically polarized radiation is a minimum and the phase change on reflection is

less than 180° . If the surface-reflected signal is attenuated there will not be complete destructive interference between the direct and an attenuated reflected wave, and the decrease in sea echo with decreasing angle will not be as great as with horizontal polarization. For this reason, when the Brewster angle is about the same as the critical angle, the effect is to move the apparent critical angle to a lower value. This could possibly account for the observation that the interference region with vertical polarization occurs at lower angles than with horizontal polarization. If the critical angle is significantly greater than the Brewster angle the graph of σ° vs angle might have a bump in the interference region. That is, the sea echo over a limited region might increase with decreasing angle. All of the above factors can affect the transition from the plateau region to the interference region and several are polarization dependent. Thus, Eq. (6) must be viewed with caution when trying to provide a precise theoretical description of the transition from the plateau to the interference region.

Observations with high range-resolution radar systems resolve the ocean wave structure if the horizontal beamwidth of the antenna is not too wide.¹⁶ Comparisons of radar echoes with the water wave-heights as recorded by a single-post ocean wave gage show a close relationship between the water waves and the radar echo. The sea echo with horizontal polarization has a more spiky appearance than that with vertical polarization. The echo with vertical polarization is spread out over more of the wave. Simultaneous wave gage and radar echo records permit comparisons of the ocean wave spectra with the sea echo power spectra for both horizontal and vertical polarizations, Fig. 15. There is considerable similarity between the ocean wave spectrum and the radar echo spectrum with vertical polarization. The spectrum for horizontal polarization is wider than that for vertical polarization or for the ocean waves. Thus the vertically polarized radar data exhibits properties more similar to data found from the ocean wave gage than does the horizontally-polarized data.

On an A scope vertical polarization produces a more noise-like display than horizontal polarization. The spikiness of horizontal polarization presents more false alarms if the sought-for target is small. A-scope displays can indicate a spiky wave-like appearance when (1) the pulse width is so short that the individual waves are resolved, or (2) when the pulse width is so large that more than one wave is included. In the latter case the spikiness is due to an interference effect from the energy reflected from the individual, unresolved scatterers and the appearance on the A scope will not, in general, correspond to the appearance of the real waves.

Observations have been made by NRL at X band of breaking waves in high-winds with the capillary waves artificially damped out by the introduction of cod liver oil on the sea surface. The breaking seemed to be undiminished by the damping of the smaller capillary waves. It was observed that individual spiky echoes of short duration appeared within the area where the capillaries were diminished. These echoes apparently were due to waves breaking. More of these individual short-duration echoes occurred on horizontal than on vertical polarization. For high sea states, sea echo near the horizon at angles well below the critical angle showed the same peak values for both polarizations; but since there were more individual echoes on horizontal polarization, the average value of the sea echo was greater than for vertical polarization in this instance.⁵²

The behavior of circularly polarized radar echoes can be qualitatively inferred from the behavior of vertical and horizontal polarization.⁵ When there are significant differences between horizontally and vertically polarized echoes as sometimes reported at low grazing angles and lower frequencies, the echo returned when a circularly polarized wave is transmitted would be expected to be primarily vertically polarized since the echo with vertical polarization is greater than with horizontal. This might explain experimental data^{30, 66} reported at X band at low grazing angles that shows $\sigma_{RV}^{\circ}/\sigma_{RH}^{\circ}$ to be nearly equal to $\sigma_{VV}^{\circ}/\sigma_{HH}^{\circ}$. (The subscript R = right-hand circularly polarized radiation and L = left hand.)

Long³¹ reports measurements of sea echo at C band and K_a band where either vertical or horizontal polarization were transmitted and simultaneously both vertical and horizontal components were received. Data was obtained for grazing angles between 1.5° and 4.0° for which, it was said, σ° was not found to be strongly dependent on angle. Because of reciprocity, the instantaneous values of the depolarized echoes, σ_{VH}° and σ_{HV}° , should be equal. For the depolarized echoes, the sea echo was found to vary approximately as the cube of the wind speed but there was no direct correlation with wave height. This applied to wind speeds from 3 to 20 knots and wave heights from 0.3 to 4.1 feet. From these experiments Long suggests that the wind-generated ripples are the major cause of the depolarized echo.

5. FREQUENCY

Figure 7 and the discussion of sea echo in the preceding sections included the effects of frequency. This section attempts to summarize the chief factors affecting sea echo that can be attributed to the radar frequency. The frequency dependence of sea echo is difficult to determine precisely. To avoid variations inherent in time-sequential measurements,

simultaneous measurements should be made of the same patch of ocean at different frequencies. This is seldom done. Another factor sometimes causing confusion is the fact that the frequency dependence is a function of the polarization and the angular region over which the sea is viewed. Also, the natural spread in the experimental data is often greater than the variation one is looking for with frequency. In this section, the frequency dependence will be discussed for each of the three major regions identified with the viewing angle: quasi-specular, plateau, and interference. One conclusion reached is that there is no simple frequency dependence and that attempts to find simple relationships are not likely to succeed.

At normal incidence in a perfectly smooth sea, the radar sees its image in the water and σ^0 is proportional to the gain of the measuring antenna. Consequently the apparent frequency dependence at normal incidence over a perfectly smooth sea corresponds to the change in the measuring-antenna gain with frequency. The gain, and therefore σ^0 , varies according to theory as f^2 . This is an unusual case, however, with little practical interest since the sea is seldom perfectly smooth at radar frequencies. At near normal incidence in a rough sea where the backscattering is determined chiefly by the mean slope of the waves, there should be little dependence of the sea echo with frequency, provided the radar wavelength is small enough to consider the scattering as being described by geometrical optics. Experiments seem to verify this. (Some frequency dependence at normal incidence might be expected at frequencies above X band where the surface roughness caused by capillary waves is comparable to the RF wavelength.)

In the interference region, the clutter coefficient decreases rapidly with decreasing angle and according to Katzin¹⁷

$$\sigma^0 \sim \left(\frac{\varphi}{\varphi_c} \right)^4 \quad (7)$$

where φ_c is the critical angle. This is based on the simple model of interference between the direct and scattered wave. Substituting Eq. (6), the critical angle, into Eq. (7) predicts σ^0 to vary as f^4 in the interference region. (Although this result is widely quoted there is little experimental verification.) These relations apply primarily to horizontal polarization and do not take into account the shadowing and other factors mentioned in the preceding section which can occur at low grazing angles. The Brewster angle for vertical polarization is also frequency dependent.

The frequency dependence in the plateau region has been stated to vary anywhere from f^0 to f^4 , depending on the particular experimenter, with a linear dependence being a frequent choice. For vertical polarization the f^0 dependence appears to apply in the plateau region, for frequencies below X band.¹⁹ The linear dependence might approximate the variation obtained with horizontal polarization over a limited range of angles in the plateau region.

Many attempts have been made to find a simple law to describe the variation of σ^0 with frequency.^{7, 18} Figure 7, which presents a composite of data, illustrates the difficulty of trying to establish a single, general relation for the frequency dependence. If a simple law is to be specified, the conditions under which it applies must be carefully defined.

At frequencies above X band the capillary waves have a significant affect on sea echo. Below C band the capillary waves are probably too small compared to the radar wavelength to play as major a role as they seem to do at the higher frequencies. Thus it would not be surprising to find σ^0 behaving differently at frequencies well above X band (millimeter waves) as compared to the lower frequencies. Grant and Yaplee⁹ show a frequency dependence from $f^{1.4}$ to $f^{2.1}$ for frequencies ranging from X band to K_a band. Other measurements²⁰ from 10 to 50 GHz show σ^0 to be nearly independent of frequency but at an absolute level higher than other experimenters report at X band. Thus, on the basis of limited data one might conclude that the sea echo increases above X band.

Measurements of sea echo at laser frequencies have been reported using a 20 nsec pulse laser at 1.06 microns wavelength with a beam divergence of 6 mrad.²¹ Flight tests over water gave an average value of $\sigma^0 = -8.3$ db for "international sea states one through three" at normal incidence and $\sigma^0 = -6.2$ db for calm water. It is stated that such results suggest that at this wavelength the ocean is neither a Lambert diffuse target nor a specular mirror-type scatterer, but rather some combination of the two if the transmitter beam divergence is sufficient to illuminate a homogeneous area of sea surface.

6. OTHER FACTORS

Rain. Rain, snow, and ice can smooth ocean waves. It has been observed that rain dampens the capillary wave structure and reduces σ^0 at microwave frequencies. Measurements of sea echo in rain can give misleading values if the reflection from the rain is included with the sea echo measurement.

Contaminants. Ocean contaminants such as oils can dampen ocean waves. The effect of oil contaminants on the radar sea echo return at microwave frequencies can be quite large. PPI displays with high resolution X-band radar often show dark areas (absence of radar echo) in the vicinity of small boats, indicating the leakage of oil. Debris on the ocean surface can increase the echo.

Pulse Length. When the resolution cell of the radar is less than the wavelength of the sea, the radar can resolve the ocean waves. The resolution of the waves depends on both the range and angle resolution of the observing radar. Since 15 knot winds generate waves greater than 100 ft in length, pulse durations less than 0.1 microsecond will usually resolve the waves if the beamwidth is not too wide and if the waves are not too short-crested. As the pulse length becomes long compared to the water wavelength, the echo begins to look much more like receiver noise. Many observers refer to it as being more "spiky" (especially for horizontal polarization).

False Alarms. There are many things in the ocean which tend to affect the backscatter in addition to the waves. These effects could appear to a radar as a target and might thus create false alarms. Breaking water, for instance, results in spikes of echo which can interfere with the detection of desired targets. Objects floating in the water can contribute to the sea echo and can cause erroneous measurement of the natural sea clutter. Fish or schools of fish breaking water and flights of birds have been observed to produce discernible echo signals. Rain and localized clouds often produce effects which appear as targets or they can change the sea echo character. The combined effect of all of these sources is to produce large signals compared to the surrounding sea echo which occur infrequently but in some cases often enough to produce false targets. As indicated later in this report, the statistical distribution of sea echo shows higher tails than described by a Rayleigh distribution, especially with short pulse waveforms. This can result in a high false alarm rate if the radar were designed for Rayleigh statistics instead of the measured statistics.

Shadowing. At low grazing angles the dominant contribution to the backscattered signal generally is from the side of the wave nearest the radar. The back surface is in the shadow. Also, smaller waves can be shadowed by the bigger waves. Thus shadowing can affect the scattering behavior of sea surfaces. A shadowing function was suggested by Beckmann³⁴ for scattering by random rough surfaces. He defined it as the ratio of the illuminated area to the total area. This function is unity at normal incidence and zero at zero grazing angle. Its variation with angle is qualitatively like that of the sea echo. However it has been argued^{35, 45}

that this approach to accounting for shadowing over-estimates the effect by a considerable amount since the scattering elements responsible for the major portion of the backscatter are not as likely to be in the shadow as an arbitrary point on the surface.

The imaging of sea echo as a wave-like pattern on a radar display probably is enhanced by the shadowing effect in many instances.

Fluctuations. Sea echo can exhibit large, rapid fluctuations in amplitude. The echo from the sea consists of the contributions from the many individual scattering elements within the radar resolution cell. Motion of the scattering elements produces changes in the relative path lengths from the radar to the individual elements. Therefore changes in the relative phase differences occur among the individual echo contributions to yield a resultant echo signal that varies with time. The range of fluctuations is described statistically by a probability density function $p(\sigma)$ such that $p(\sigma)d\sigma$ is the probability that the resultant cross section will be between the values σ and $\sigma + d\sigma$. The Rayleigh probability density function has often been used to describe the fluctuation of the sea echo as well as other distributed targets. It is applicable when the echo is the result of the contributions of many independent scatterers of approximately equal cross section. This not only seems to be a reasonable model for a distributed clutter target but it is convenient to handle mathematically. The Rayleigh probability density function (pdf) is

$$p(\sigma_c) = \frac{1}{\sigma_{av}} e^{-\sigma_c/\sigma_{av}} \quad (8)$$

where σ_{av} is the average value of the clutter cross section σ_c .

Experimentally measured statistics of sea echo fluctuations do not always follow the Rayleigh description. In some cases sea echo has been observed to have a higher probability of obtaining large values than would be indicated from Eq. (8), that is, the actual pdf's do not decrease as rapidly for increasing σ as does the Rayleigh. This is especially true of measurements taken with high resolution radar.³⁶ George and others have suggested that the data tends to follow a log-normal pdf rather than the Rayleigh pdf.³⁷ The pdf for clutter cross section σ_c that is log-normally distributed is

$$p(\sigma_c) = \frac{1}{\sqrt{2\pi} \sigma_s \sigma_c} \exp \left\{ -\frac{[\ln(\sigma_c/\sigma_m)]^2}{2 \sigma_s^2} \right\} \quad (9)$$

where σ_m = medium value of σ_c and σ_s = standard deviation of $\ln \sigma_c$ (natural logarithm). The log-normal distribution generally has higher "tails" than the Rayleigh and helps account for a higher false alarm rate than normally expected if the echo were governed by Rayleigh statistics. The log-normal pdf requires the specification of two parameters (the median and the standard deviation) instead of the single parameter (average value) of the Rayleigh. It is thus more difficult to analyze and interpret than the Rayleigh model. Also, there is no satisfactory physical model of the sea which leads to the log-normal distribution as there is with the Rayleigh.

Trunk has pointed out that the tails of the log-normal distribution are higher than experimental measurements and that a contaminated-normal distribution provides a better fit.⁵³ The contaminated normal is described by the sum of two (or more) normal distributions of different parameters, as in Eq. (10).

$$P_{\gamma, K} = \frac{(1-\gamma)}{\sqrt{2\pi}\sigma} \exp\left(-\frac{x^2}{2\sigma^2}\right) + \frac{\gamma}{\sqrt{2\pi}K\sigma} \exp\left(-\frac{x^2}{2K^2\sigma^2}\right) \quad (10)$$

where γ is the contamination fraction, K is the ratio of the standard deviations of the Gaussian densities, and σ is the standard deviation of the uncontaminated distribution, that is when $\gamma = 0$.

Figure 16 shows examples of the measured probability distribution function of sea echo obtained with high resolution radar. For comparison the Rayleigh, log normal and the contaminated normal probability distributions are shown.

When the distribution of sea echo has high tails, Trunk⁵⁴ has suggested that the median-value detector may be more efficient than the mean-value detector.

Doppler. The fluctuations observed in the sea echo may also be considered to result from the doppler frequency shift produced by the motions of the individual scatterers. The different doppler shifts beat with one another to generate the observed fluctuation. The analysis of the amplitude fluctuations as the superposition of the doppler contributions is equivalent to the analysis assuming the superposition of signals with time varying phase shifts caused by the relative motions. Measured spectra of sea echo amplitude fluctuations at microwave frequencies show the spectral width to be proportional to the radar frequency, as it should be if due to a doppler effect. The spectral width corresponds to a few

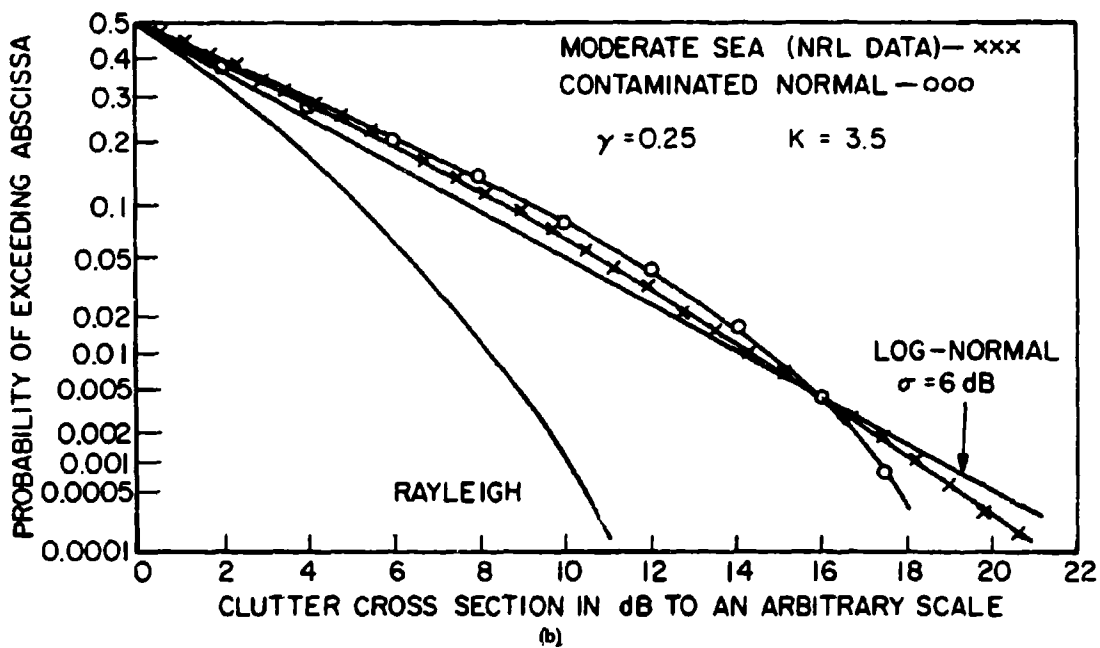
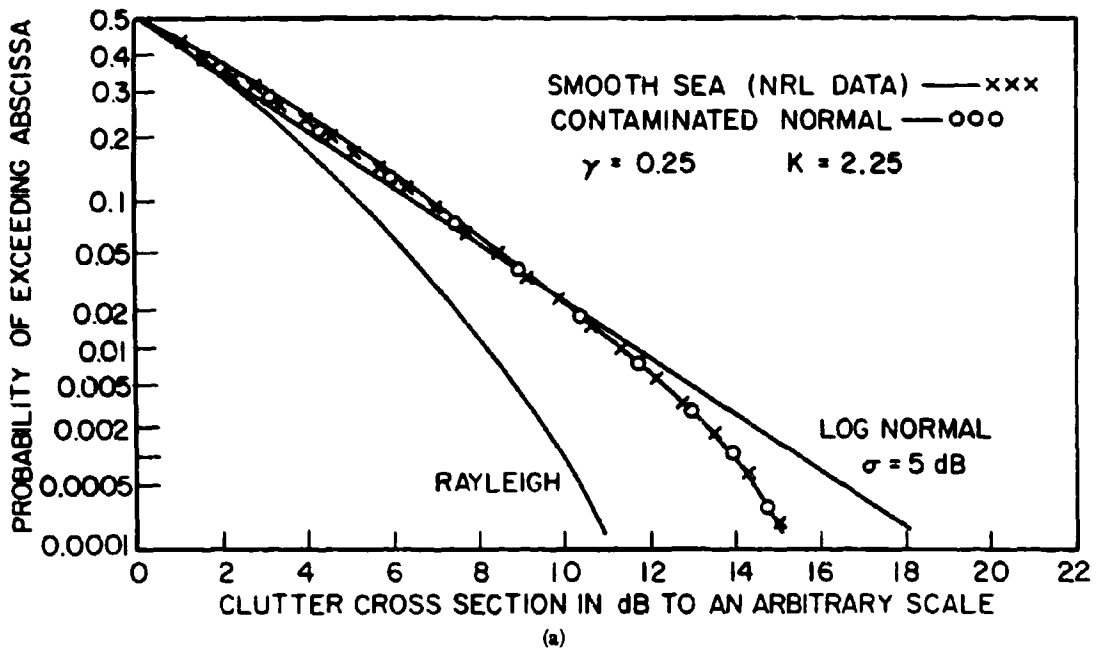


Fig. 16 - Measured probability distribution at X band compared with the Rayleigh, log-normal and contaminated normal distributions. (a) "Smooth sea," (b) "Moderate sea."

knots velocity. Figure 17 is an example of a typical frequency spectrum measured at X band. According to Goldstein⁷ the measurements available to him did not seem to indicate any significant variation in the spectra with roughness of the sea. Measurements by Hicks et al⁴² indicate the spectral width of the clutter to be approximately proportional to the wind speed.

Amplitude fluctuations are measured with a noncoherent radar. They show the spread in doppler but not the center frequency of the doppler itself. Measurements of the doppler with a coherent system give the average velocity. The doppler shift corresponds to a few knots (the spread is also a few knots). This velocity is considerably less than the actual wave velocity and is thought to correspond to the velocity of the water particles which is also much smaller than the wave velocity.

Wright⁵⁸ has observed that the doppler spectrum of mechanically generated waves in a water wave tank are sharply peaked at an angular frequency ω given by

$$\omega^2 = gk + sk^3 \quad (11)$$

$$k = 2k_0 \cos \varphi \quad (12)$$

where g = acceleration of gravity, s = the ratio of surface tension to water density, k = water wave propagation constant = $2\pi/\lambda_w$, λ_w = water wavelength, k_0 = radar propagation constant = $2\pi/\lambda_r$, λ_r = radar wavelength, and φ = grazing angle. (At low grazing angles this implies that $\lambda_r \approx 2\lambda_w$.) With wind generated waves the doppler spectra are very much broadened and peak at a frequency related to the grazing angle in a similar manner, but the relation depends on wind speed. Little apparent difference was noted in these experiments in the shape of the spectra for horizontal and vertical polarization.

At the lower frequencies (long wavelengths) the small scale structure seems to play less of a role than at microwave frequencies and the large gravity waves are probably the primary scatterers. The doppler shift at these lower frequencies (HF, VHF, and UHF) correspond to the water wave velocity rather than the particle velocity that is characteristic of microwave sea echo.

Crombie³⁸ observed that at HF (13.56 MHz) the backscatter was greatest for ocean waves moving radially with respect to the radar and of length about half the radar wavelength. The latter is the same as the condition given by Eq. (12), or

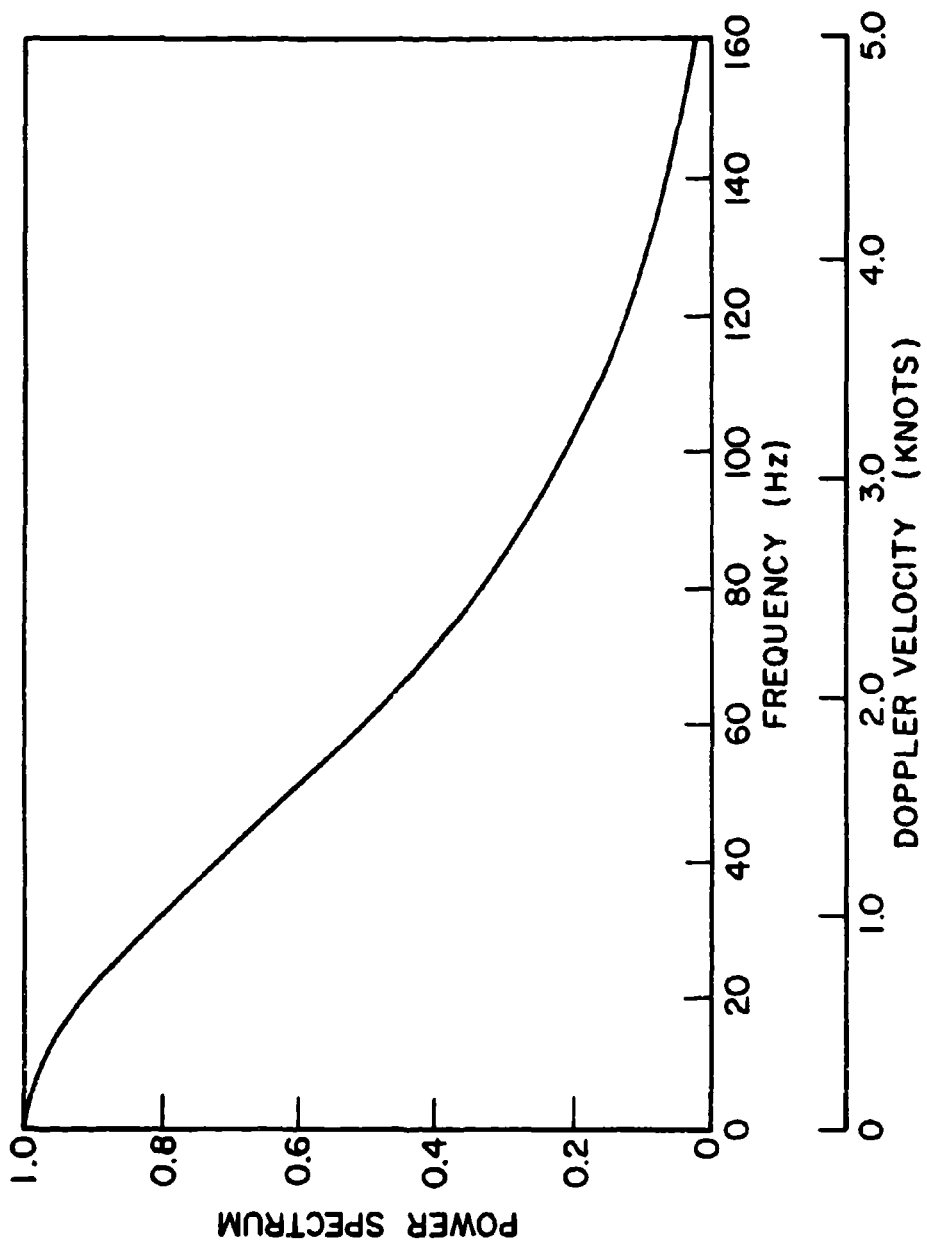


Fig. 17 - Typical power spectrum of sea echo at 3.2 cm wavelength.
 (From Goldstein, 7)

$$\lambda_r = 2\lambda_w \cos \varphi \quad (13)$$

where λ_r = radar wavelength and λ_w = water wavelength. The ocean consists of many component waves as mentioned in Sec. 1. If the spectrum of the sea contains a component that meets the conditions stated by Crombie it will produce backscatter. There are actually two components that can meet these requirements and they will be of velocity $\pm v$, that is, one approaches the radar traveling radially and the other recedes. The two components are not necessarily of equal amplitude. They might differ by as much as 10 db. From classical ocean wave theory (ignoring the effect of surface tension), the velocity is

$$v = \left(\frac{g \lambda_w}{2 \pi} \right)^{\frac{1}{2}} \quad (14)$$

From Eqs. (13) and (14) the doppler shift is

$$f_d = \pm \frac{2v \cos \varphi}{\lambda_r} = \pm \left(\frac{g \cos \varphi}{\pi \lambda_r} \right)^{\frac{1}{2}} \quad (15)$$

This has been verified by many measurements reported from HF to UHF.^{39, 40} At times a component of the spectrum at the transmitted frequency has also been observed experimentally. (This might be due to the unintentional inclusion of some land echoes obtained from the sidelobes.) At HF the doppler frequency shift is about 0.5 Hz and the measured widths of the spectral lines are reported as 0.01 to 0.03 Hz. Note that the doppler-shifted frequency of Eq. (15) varies as the square root of the radar frequency (inverse of λ_r) rather than directly with frequency as is more usual with the doppler shift.

Thus the sea echo has a very distinctive doppler spectrum at the lower frequencies as compared to the spectrum of land echo. The echo consists of two frequency shifted components centered about the location of the carrier by an amount given by Eq. (15). There is no component of the returned signal at the carrier frequency unless it is inadvertently obtained from land backscatter illuminated by the main beam or the sidelobes. These two frequency components result from the selective scattering from those sea waves whose lengths are half the radar wavelength and which are traveling in a radial direction. It has been demonstrated⁵⁵ that by taking advantage of the inherent difference in the sea and land spectra, the echo from the sea using ionospherically propagated HF can often be distinguished from land echoes and that it is possible to generate a map of land-sea boundaries by this technique.

The expression for the shift in frequency due to wave motion as given in Eq. (15) applies at the longer wavelengths (HF, VHF, UHF) and for low winds. For shorter wavelengths (C band and above) the surface tension must be included as in the second term of the righthand side of Eq. (11). In the case of high winds an additional frequency shift is said to take place due to the wind drift of the surface layer of water.²⁸ This drift velocity is denoted as v_w and makes an angle θ relative to the direction of the radar radiation. The frequency shift is then given by

$$f_s = \pm \sqrt{\frac{g \cos \varphi}{\pi \lambda_r} + \frac{16 \pi g \cos^3 \varphi}{\lambda_r^3}} + \frac{2 |v_w \cos \theta|}{\lambda_r} \quad (16)$$

where the symbols have been defined previously. The absolute value of $v_w \cos \theta$ is present in Eq. (16) since the phase velocity of the ripple or capillary waves and the wind-drift velocity of the surface layer v_w always coincide in direction.

Figure 18 shows a plot of the radical portion of Eq. (16) for low grazing angles ($\varphi = 0$, $v_w = 0$). Note that the first term (gravity waves only) dominates at radar frequencies below L band. For comparison the doppler frequency shift ($2 v/\lambda$) for velocities of 1 and 10 knots are drawn as the dashed lines. These might represent the third term of Eq. (16) or they can be thought of as the doppler shift produced by a surface target so as to illustrate the problem of an MTI radar that must separate the doppler frequency shift of the desired target from that of the sea echo. Measurements of sea echo fluctuation made during WWII indicate that at S band and above the frequency shift seems to be dominated by the third term of Eq. (16) since the power spectra were relatively independent of the product $f_s \lambda_r$, as would be if a true doppler shift.¹³

Pidgeon⁵⁶ in conducting experiments at C band (5.7 cm wavelength) found that the mean doppler shift for horizontal polarization is 2 to 4 times greater than that for vertical polarization for the same or similar wind and wave conditions. He concludes that the vertical polarization doppler shift is dependent on the wave height and is directly related to the orbital velocity of the gravity waves. On the other hand, the horizontal polarization doppler shift depends on both the wave height and the wind speed and is related to the motion of a surface layer of the sea. The velocity of this surface layer is said to be the sum of (1) the orbital velocity of the sea moving beneath the layer and (2) a velocity that is a function of the wind. For both polarizations the mean doppler shift varies as the cosine of the angle between the wind and wave direction (assumed the same) and the radar propagation direction. The spectral

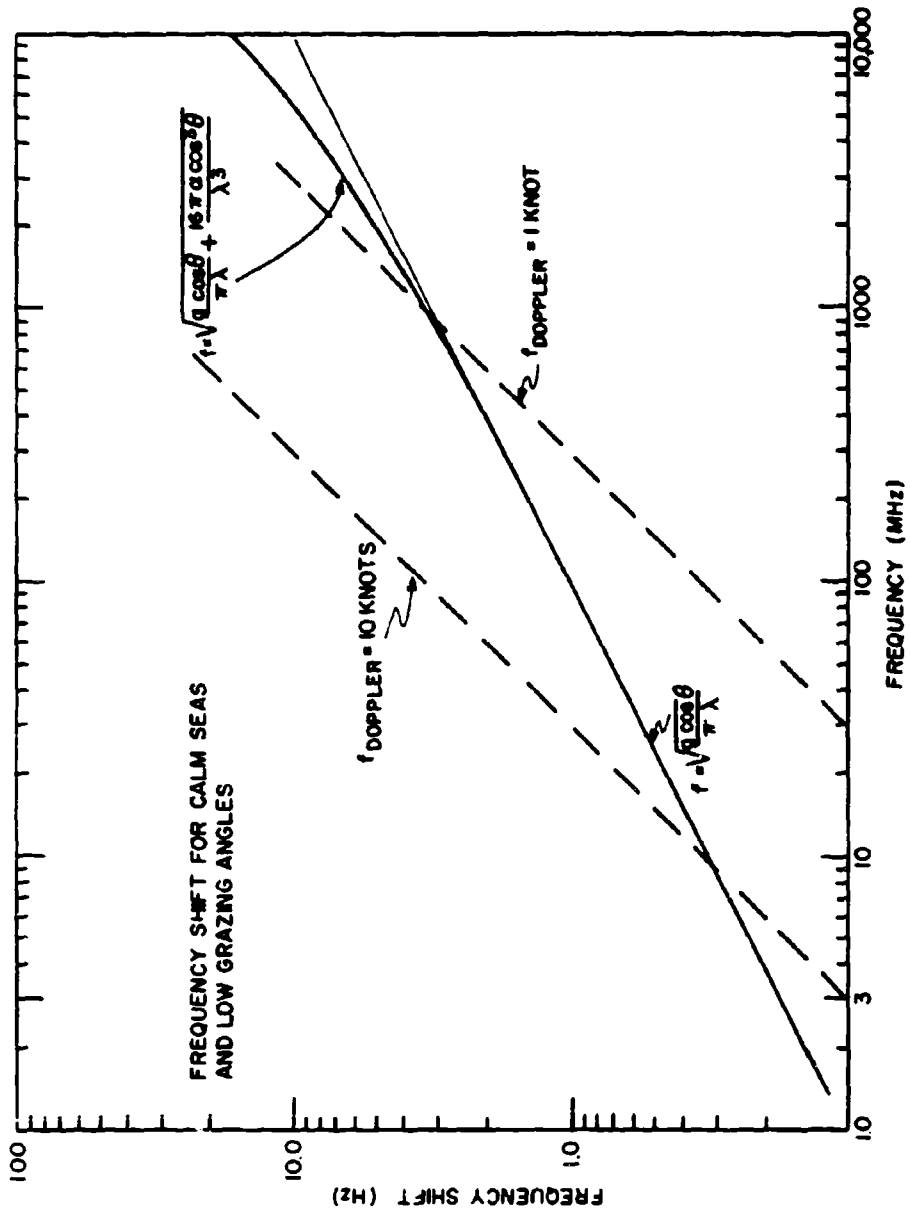


Fig. 18 - Frequency shift of the sea echo for calm seas and low grazing angles. (Plot of Eq. (16) with ϕ and $v_y = 0$.)

width, however, is independent of this viewing angle and polarization. For small grazing angles, the doppler shift and the spectrum bandwidth are independent of the grazing angle. For both polarizations, the spectral width is directly dependent on the mean doppler shift obtained looking into the wind and waves.

Bass et al³⁰ state that the spectral width depends on the sea condition and increases as the roughness increases. To quote: "The physical nature of the spectrum widening is absolutely clear: scattering sites of the ripple (the scattering is resonant!) being imposed on a large wave, move relative to the [radar] which leads to the doppler frequency-shift in addition to the frequency displacement" [described by Eqs. (11) and (12)]. They also found that the spectral width, as well as the frequency shift in the case of heavy seas depended upon the angle between the directions of the radiation and the wind. This is in disagreement with Pidgeon's observations of the spectral width. As mentioned previously Hicks et al⁴² also observed the spectral width at X band to be approximately proportional to wind speed.

Trapping. It has been observed that when a microwave radar is sited sufficiently close to the water surface, the radiation can be trapped in a duct and propagation can be obtained with low loss.⁸³ This duct is a result of evaporation which causes the index of refraction of the lower part of the atmosphere to decrease with increasing height. Trapping is apparently quite effective at X band and can increase the radar range substantially. Trapping in the evaporation duct is weaker the lower the frequency. This increased range due to trapping is important in trying to see small targets low on the water. However, one might also suspect that trapping could lead to erroneous measurements of σ^0 at X band with low grazing angles if it is not properly taken into account.

7. SEA ECHO THEORY

A clear understanding of the physical mechanism causing radar sea echo permits intelligent design of radars for the detection of targets on or near the surface of the sea. If the precise physical nature of the sea were known, classical electromagnetic scattering theory could be used to compute the nature of the radar echo. (Although the procedure might be "straightforward" it would not necessarily be "simple.") It has proven difficult to provide a realistic model of the sea that can account mathematically for all observed experimental data. There are several reasons for this situation. The sea surface is ever-changing and is affected by many forces. However, the dynamic nature of the sea should not in itself prove a fundamental limitation since statistical methods might

be applied as has been done successfully by electrical engineers in dealing with receiver noise or fluctuating target echoes. To understand the sea as a radar target one must understand something about the hydrodynamics of the sea surface and the nature of the coupling between the sea and the wind. The theorist must have a knowledge of electromagnetic scattering theory and the theory of ocean surface waves. The problem is made difficult by the fact that the oceanographers who study waves on the sea are generally interested in water wavelengths considerably longer than those that affect radar. As mentioned several times in this report, radar scatter is primarily determined by the waves of water wavelength comparable to the radar wavelength. The above difficulties are in addition to the many experimental factors mentioned in Sec. 1 that result in experimental measurements with large variance and that make attempts to check theory with experiment a frustrating task.

Figure 6 showed three regions into which the behavior of σ^0 as a function of grazing angle could be categorized: the interference, plateau, and quasi-specular regions. Although the goal is to identify a single mechanism that correctly describes the radar backscatter for any grazing angle, it has usually been easier to consider models applicable to each region separately. In brief, it seems that for microwave frequencies observing in the quasi-specular region, scattering can be "explained" as being due to facets large compared to the radar wavelength. In the plateau region the scatterers are the facets or capillary waves that are comparable in size to the radar wavelength. In the interference region the vector addition of the direct ray and the ray scattered from the water surface plays the dominant role. The interference region analysis is not applicable near, at, or beyond the radar horizon where classical diffraction theory must be considered for determining propagation effects. It must also be abandoned when trapping of the radar signal takes place.

Schooley²⁷ examined limiting cases of the radar sea return. One limiting case is a perfectly smooth surface. As mentioned previously, the clutter coefficient σ^0 at normal incidence over a smooth perfectly conducting surface is proportional to the gain of the radar antenna ($\sigma^0 = G/4$). Thus a thirty db gain antenna (beamwidth ≈ 5 to 6°) would indicate a value of $\sigma^0 = 24$ db. Over water which is not a perfect conductor, this will be reduced by the magnitude of the reflection coefficient. At X band the reflection coefficient is about 0.75 at normal incidence so that the value of σ^0 is reduced by about 2.5 db. The reduction is less at lower frequencies.⁶ The decrease in σ^0 with angle from the normal is quite rapid. A rough surface according to Lambert's law is one which scatters, per unit angle, a power proportional to the cosine of the acute angle between the direction of the scattering and the normal to the surface at the unit area.

This results in $\sigma^0 = 4 \sin^2 \varphi$ if the diffuse surface is perfectly conducting. (Schooley also considered a rough surface described by $\sigma^0 = 2 \sin \theta$ which assumes that a rough surface when illuminated by a bundle of parallel rays of fixed cross section and given total power will reradiate in the direction of the source of the rays a power per unit solid angle independent of the direction of the incident rays. This is sometimes called the "Lommel-Seeliger" scattering law. Ament⁵⁷ shows that this is an erroneous law for the rough surface even though it is found in some of the literature on backscatter.) The model of the perfectly smooth surface predicts values higher than generally observed at normal incidence and the perfectly rough surface predicts values higher than observed at angles other than normal. Thus the sea can not be simply described as being either perfectly smooth or perfectly rough.

The first models proposed for explaining sea echo were devised during World War II. Over the years there has been steady, if slow, progress toward improving the understanding of the properties of the sea as they affect the radar echo. Goldstein^{7, 13, 18} first attempted to explain sea echo by the application of diffraction theory to the large-scale sea waves, or macrostructure of the sea surface. He considered as a model a sinusoidally corrugated mirror and employed conventional physical optics techniques for analysis. The model resulted in a polar diagram for the scattered intensity like that of a grating and showed discrete peaks at the angles corresponding to the various grating lobes. Goldstein states this obviously does not correspond to the true situation.⁷ (Later work indicates that under certain conditions grating lobes in the scattering pattern do exist.³³) Davies and Macfarlane²⁹ made an attempt to consider a sufficiently irregular model by assuming the sea to consist of sinusoidal waves with successive waves having different amplitudes and wavelengths distributed according to a Gaussian law. Computations were carried out using a modified Kirchoff-principle method. Although these models gave qualitative agreement with some of the experimental data (in particular, it gave an angular dependence similar to that observed) they did not explain the differences with polarization, and the echo intensity calculated was many orders of magnitude less than measured. In hindsight it appears that the smooth surface of the sine-wave model is not realistic for microwave frequencies. It is known that a long, relatively smooth distributed target will scatter poorly in the back direction unless there are discontinuities in the target or if the surface is rough. It is interesting to note that Goldstein¹³ stated that for the theory to explain the experimental results the "maximum sea wavelength which contributes to the echo is only one-half wavelength." At microwave frequencies "these waves can thus only be small irregularities on the surface of the larger waves. In fact these correspond to ripples smaller than have been as yet observed." These ripples do exist and they can be important in radar scatter at microwave frequencies. Goldstein's interpretation of electromagnetic scattering theory was correct and it is unfortunate there wasn't better knowledge available of the ripples (capillaries) at that time. The early attempts at using

diffraction theory to explain sea echo failed because of too simple a model for the sea. Although theory indicated what the correct model should be, apparently it was not appreciated until later that waves did exist on the ocean surface that were comparable to microwave wavelengths.

Goldstein also examined the hypothesis that scattering results from spray droplets thrown up above the water surface. Droplets over the water surface could explain qualitatively the polarization effects observed experimentally at low grazing angles. It was suggested that the droplets are illuminated by a direct ray from the radar and a ray reflected from the surface of the water. These two rays combine vectorally at the water droplets. With horizontal polarization, the magnitude of the reflection coefficient is very nearly unity and the phase shift on reflection is approximately π radians. Thus at low grazing angles the two rays will destructively interfere and little or no energy will illuminate the droplets. The less energy illuminating the target, the less will be the magnitude of the echo. A similar effect occurs with vertical polarization except for the important difference that at the Brewster angle the magnitude of the reflection coefficient is less than unity so that the direct and reflected rays do not produce as complete cancellation as observed with horizontal polarization. Thus the vertically polarized waves place more of the radiated energy at low angles and will give a greater reflection than with horizontal polarization. Simple theory predicts that the echo with horizontally polarized radiation over a perfectly reflecting surface will vary as φ^4 at low grazing angles. As the sea becomes rougher the differences observed experimentally with the two polarizations become less. This is explained in the droplet theory by stating that as the sea becomes rougher the interference pattern, especially at the minima, tends to be destroyed. Since the drops are small compared to the wavelength, the droplet theory predicts that the target echo should vary as f^4 in rough weather and f^8 in calm weather. This dependence of σ^0 is not usually observed. Another reason to suspect the validity of the droplet theory is that the polarization dependence is observed experimentally to be greatest in a calm sea when there is no spray. For these and other reasons Goldstein concludes that it is "not likely that the drop mechanism represents the actual state of affairs." The major interest in the droplet theory is that it seems to explain the polarization dependence. This does not depend necessarily on the scatterers being droplets so that in seeking a better model one might look for a different type of scatterer but keep the concept of direct and reflected rays at low grazing angles.

(It might be noted in passing that, as mentioned in Sec. 4, breaking waves do cause whitecaps and spray that result in a spiky echo of short duration. Thus spray, droplets or whitecaps can produce a radar echo but they do not seem to be a major contributor to the total echo from the sea.

Although there may be a correlation between a whitecap and the appearance of a spiky echo on an A scope it is not clear whether the major contribution to the echo comes from the spray or from the very peaked crest that develops before the wave breaks.)

Katzin²⁴ advanced the suggestion that instead of droplets the scattering elements are small patches, or facets, that overlie the main large-scale wave pattern. He considered the surface of the sea to be the superposition of facets of various sizes, with orientations distributed about the main sea contour. He assumed that the phases of the signals scattered from the facets were independent and reasoned that since the values of σ^0 at low grazing angles were small (10^{-3} or less) the scattering mechanism should be rather highly directive. This suggested to him that the scattering properties of inclined flat plates (facets) be investigated. Katzin claims this theory accounts for the behavior in the interference region and the critical angle, and that it explains the approximate polarization dependence, the approximate frequency dependence and the behavior near normal incidence. It is also said to account for the spikiness observed with horizontal polarization at low grazing angles.

Katzin's facet theory failed to explain the observed upwind-downwind ratio (Sec. 3) of sea echo. Schooley¹⁴ suggests this was due to a lack of measurements of the facet size and slope distributions upon which to base calculations. As mentioned in Sec. 3, Schooley measured the statistics of the facet sizes in a laboratory water wind-tunnel and from these measurements calculated the upwind-downwind ratio as a function of depression angle at several frequencies. His results as shown in Fig. 12 were in sufficient qualitative agreement with measurements as to lend support to Katzin's facet model.

Both Schooley and Katzin assumed that the scattering from the facets was essentially independent of the polarization. Wright^{12, 50} has studied both experimentally and theoretically the scattering from capillary waves at intermediate grazing angles in the plateau region. He suggests that the elemental scatterers are more appropriately thought of as patches of water waves whose scattering properties prove to be strongly polarization dependent. Capillary waves are small wind-generated ripples of wavelength less than about one inch that ride on top of the larger wave structure. They are important to the scattering mechanism at X band and higher frequencies since the scattering is attributed to water waves of propagation constant $k = 2\pi/\lambda_w$, which are related to the microwave propagation constant $k_0 = 2\pi/\lambda_r$ by $k = 2k_0 \cos \varphi$, where λ_w = water wavelength, λ_r = radar wavelength and φ = grazing angle. Wright derived a theoretical relation for the scattering from such waves and was able to obtain good agreement between theory and experimental measurements of the variation

of σ^0 as a function of grazing angle for vertical polarization. The agreement for horizontal polarization was not as good. Wright's work is of interest since he carried out his experiments under controlled laboratory conditions in a wave tank. Although the wave tank may not represent the ocean in all respects, controlled laboratory experiments give an understanding of the factors determining the radar echo from the real ocean. Wright's application of first order (small amplitude) scattering theory appears to have been more successful than previous attempts to quantitatively associate radar sea echo to the properties of the ocean waves.

It seems to have been well established that theories describing radar scattering from the ocean must take account of the small wave structure (ripples, capillaries, facets) as well as the large wave structure. Theoretical studies^{59, 60} of scattering from rough surfaces now recognize the composite nature of surfaces like the sea and consider both the large-scale and the superimposed small scale irregularities. If the frequency is low enough the effect of the small scale wave structure should be negligible and only the large waves will affect the sea echo. This was mentioned briefly in Sec. 6 on doppler effect. At the lower radar frequencies (HF, VHF and perhaps UHF) the radar wavelengths are comparable to the water wavelengths that begin to interest oceanographers and data on ocean wave spectra including these components are more likely to be available than the spectra of the capillary waves that affect the higher microwave frequencies.

At the time of writing, much progress has been made toward understanding the physical mechanism producing sea echo and in the development of mathematical models that permit quantitative predictions of sea echo behavior and comparisons of theory with experiment. More progress is needed.

8. INFLUENCE ON DESIGN

It is not unusual for the sensitivity of a radar required to detect targets over water to be limited by the sea echo, or clutter, rather than receiver "thermal" noise. The sea echo can extend to the radar horizon which typically might be about 10 miles or more for a shipboard radar and much farther for an airborne radar. The design philosophy of a clutter-limited radar can be decidedly different from one that is noise limited. The term sea clutter is used in this section for sea echo to emphasize that the echo from the sea is a nuisance that "clutters" the radar with undesired targets that can hinder the detection of the desired targets. In such a situation the aim of the radar designer is to reduce the amount of clutter with which the desired target must compete by resolving the target in doppler frequency (MTI), range (wide bandwidth), and angle (narrow beamwidth). Improvement of the detectability of targets in clutter

can be obtained by properly employing scan-to-scan integration and pulse-to-pulse frequency agility so as to utilize independent samples of clutter echoes. Techniques such as logarithmic receivers with FTC (Fast Time Constant), adaptive video thresholding and similar methods do not provide enhancement of the target-to-clutter ratio. They do prevent overloading of the receiver or display and are often helpful for that reason.

Range Equation for Clutter. The maximum range R_{\max} of a pulse radar viewing clutter at low grazing angles can be expressed as

$$R_{\max} = \frac{\sigma}{(S/C)_{\min} \sigma^{\circ} \theta_b c (\tau/2) \sec \varphi} \quad (17)$$

where σ is the target cross section (A summary of the cross section of sea targets is given in Ref. 65.), $(S/C)_{\min}$ = minimum signal-to-clutter ratio necessary for reliable detection, θ_b = azimuth beamwidth, c = velocity of propagation, τ = pulse width, and φ = grazing angle. This equation is different from the normal radar range equation that assumes the sensitivity is limited by noise rather than clutter. Note that the range as given by Eq. (17) does not depend explicitly on the transmitted power. An increase in power increases the echo from the target, but it also increases in like amount the echo from the clutter. The transmitted power does not appear in the range equation so long as the power is large enough to make the clutter echo at the receiver significantly larger than the receiver noise. For simplicity here the receiver noise is ignored, but it cannot be neglected at long ranges or when the clutter coefficient σ° is small. (More precisely, the clutter-plus-noise power should be considered rather than clutter only or noise only.) The antenna gain and effective aperture do not appear explicitly in Eq. (17) except for the azimuth beamwidth θ_b .

A narrow beam is desired so as to reduce the size of the clutter patch with which the target echo must compete.⁶⁴ A narrow beam implies a high gain. For a given size aperture, the higher the frequency the higher the gain. This reasoning might lead to the selection of a high radar frequency for a radar that must operate in sea clutter, but it must be cautioned that the higher the frequency the greater is the value of σ° , especially if the polarization is horizontal. Generalities cannot be offered in selecting the radar frequency since one must carefully consider factors not given explicitly in the simple radar equation.

The pulse width of the radar should be small to achieve long range in clutter. This might seem strange since the shorter the pulse the less the energy contained in the signal. Contrary to the experience with noise-limited radars, the lesser energy in a short pulse does not degrade detection

as long as the assumptions contained in Eq. (17) apply, in particular that the clutter echo is large compared to the receiver noise. Pulse-compression waveforms can be used to achieve the benefit of the clutter reduction afforded by a short pulse as well as the added energy in the transmitted waveform to extend the range of the radar when not clutter limited. Too small a resolution cell can sometimes result in a degradation of detection if the resolution of the display is not as good as that of the radar waveform. A collapsing loss can result. There is also the problem inherent with high resolution radar that there may be too much information for an operator to handle effectively. Automatic processing might be employed to relieve the burden on the operator but practical difficulties of equipment implementation might arise if the bandwidth associated with high resolution signals is too wide.

The factor $(S/C)_{\min}$ is analogous to the minimum detectable signal-to-noise ratio of the conventional noise-limited radar equation. To specify the signal-to-clutter ratio for a given probability of detection and average false alarm time requires a knowledge of the statistics of the clutter, in particular the probability density function and the correlation of the echo with time and space. The statistics of real sea clutter are not as well described mathematically as those of thermal noise. One of the simplest statistical models is to assume the clutter echo is composed of a large number of independent scatterers of approximately equal size. This clutter model is described by the Rayleigh probability density function. The Rayleigh model is convenient mathematically and it is the same probability density function that describes the envelope of the noise from a narrow-band filter. There is experimental evidence, however, which indicates that in some situations the sea clutter statistics are not faithfully described by a Rayleigh distribution but show higher likelihood of obtaining a large value of clutter than would be given by a strictly Rayleigh distribution.³⁷ (See discussion of Fluctuations in Sec. 6.) When no precise information of the clutter statistics are available (or more correctly, the statistics of clutter-plus-noise) the radar designer is quite likely to take as approximations to the correct value for the signal-to-clutter power ratio the values of signal-to-noise ratio (S/N) , visibility factor (V_0) or ratio of signal-energy-to-noise-power-per-unit-bandwidth (E/N_0) .

The terms probability of detection, probability of false alarm and average time between false alarms have well understood meanings when the target signal competes only with receiver noise. They are less well determined when detection is limited by clutter. In addition to not knowing precisely the probability density function for a particular sea condition there is also the problem that the distribution is dependent on the direction of the wind and it varies with time at any point in the ocean and can be different at any one time at different locations. Thus the clutter statistics in a particular area are not necessarily stationary as can

generally be assumed for the statistics of receiver noise. The clutter statistics will also depend on the general area of the world being considered. A shipborne radar in the Mediterranean Sea in the summer where the seas are relatively calm is likely to perform far better than a similar radar in the North Atlantic during winter. A radar that is operating poorly because of high sea conditions is likely to continue to operate poorly until better sea conditions prevail. Thus one must treat with caution concepts such as the probability of detection developed for the noise-limited situations when applied to the radar limited by sea clutter. (Nevertheless, the radar designer must often employ the concepts developed for noise-limited radars when no better information exists.) The oceanographer has data on the sea conditions for various parts of the world³ but these are not always easy to convert to values of σ^0 , the parameter of interest to the radar designer.

The sea at any particular point is ever changing, but during the usual observation time of a scanning radar (perhaps a fraction of a second) the sea is essentially "frozen." Thus the sea clutter will tend to be correlated from pulse-to-pulse throughout the scan so that integrating a number of pulses does not necessarily improve the signal-to-clutter ratio as would integrating pulses in a noise-limited situation where the noise is independent pulse-to-pulse. The decorrelation time of sea echo is stated by Croney⁶¹ to be about 0.01 sec at X band. He shows that improvement in signal-to-clutter can be achieved by using a rapidly rotating antenna (600 rpm with a prf = 5000 Hz in his experiments) so that integration of scan-to-scan decorrelated returns is practical. Instead of sweeping the antenna slowly so as to obtain a large number of pulses per target per scan it is better to scan rapidly and to integrate the same total number of returns from scan to scan. The integration is performed on a cathode-ray-tube display in the examples investigated by Croney.

The decorrelation time of the order of 0.01 sec mentioned above is apparently due to the motion of the water surface causing the scattering. If this is the case then the decorrelation time might be expressed as $T_d > \lambda/4v$ where λ is the radar wavelength and v is the velocity of the scatter. The correlation time thus should be proportional to wavelength. However the velocity of the wave is proportional to the square root of the water wavelength (Eqs. (1) and (2)) so that as the radar wavelength increases the correlation time increases, but at a slower rate than that given by a linear law. Another factor to consider is that Eqs. (1) and (2) relating velocity and wavelength apply to gravity waves and not to the capillary waves experienced at X band. Perhaps an upper bound to the decorrelation time can be had from an examination of the solid curve of Fig. 18 giving "doppler" frequency shift as a function of frequency. The inverse of this

frequency shift may be considered a measure of decorrelation time. To account for a decorrelation time of about 0.01 sec at X band (frequency shift of 100 Hz) requires that the scatterers be driven by a wind of no less than several knots.

In addition to the normal sea clutter there are often large peaks of sea echo (perhaps corresponding to a radar cross section of 1 sq m or more) that might be caused by breaking waves. The correlation time of these spike-like echoes is determined by a different mechanism than the simple water motion described above. These echoes might persist for several seconds at X band.

In the conventional noise-limited radar equation, the range enters as the fourth power. Therefore changes in such factors as the transmitter power, noise figure, required signal-to-noise ratio, and target cross section do not have as significant an effect on the range as do similar changes in the factors of the clutter-limited equation where the range is to the first power. For example, if the actual target cross section is 3 db less than that assumed for calculating the range in a noise-limited case, the actual range will be about 84% of that predicted. In the clutter-limited case of Eq. (17) the actual range would be half that calculated. The same holds true of the other parameters. One of the most uncertain factors in the clutter-limited range equation is the value of σ^0 . An uncertainty of only 3 db in its value is considered good. However, it is not unusual to find differences of 10 db in values of σ^0 obtained under seemingly identical experimental conditions. The radar designer when possible must allow for these uncertainties with conservative design. Because of the linear range dependence, a clutter-limited radar is likely to experience wider fluctuations in performance than a noise-limited radar.

Equation (17) is an approximation for low grazing angles. At or near normal incidence, the applicable equation is

$$R_{\max}^2 = \frac{\sigma G_t \sin \varphi}{\sigma^0 4 \pi (S/C)_{\min}} \quad (18)$$

where G_t = transmitting antenna gain and the other factors have been defined previously.

A civil marine radar must see stationary targets or targets moving too slowly relative to the motion of the sea for effective MTI or discrimination by doppler. To be detected, their echoes must be significantly larger than the echoes from the sea. As an example of the clutter magnitude, assume

a beamwidth of one degree, a pulse width of one microsecond, and the range of interest to be five miles. The size of the clutter patch illuminated by the radar is approximately $R \theta_b c \tau / 2 = 5 \times 1852 \times (1/57.2) \times 150 = 24000 \text{ m}^2$. If the clutter coefficient σ^0 is -40 db and if the signal-to-clutter ratio must be 16 db for reliable detection, the minimum size target that can be discerned is about 100 m^2 . At this range such a radar will easily see a merchant ship but would probably not see a small fishing vessel or unaugmented buoys.

Polarization Choice. Horizontal polarization is generally chosen for civil marine radars since sea clutter is usually less with horizontal polarization. However, for targets very low on the water vertical polarization might sometimes result in better signal-to-clutter ratio and is likely to produce fewer false alarms.

As was mentioned in Sec. 3, the appearance of the radar display is different for the two polarizations when viewing the sea at low grazing angles. Vertical polarization produces a more noiselike appearance and seems to be reflected from more of the wave than horizontal polarization. The appearance of horizontal polarization is spikier and although its average level is higher, the spiky nature of the return can be comparable to or larger than the average level of vertical polarization. The spikier nature of the clutter makes it more difficult to distinguish real targets from the false alarms generated by the sea echo even though the average value of σ^0 for horizontal polarization may be smaller.

At the present time there appears to be contradictory advice as to the best polarization for detecting small targets in sea clutter. Some experiments comparing the two polarizations seem to indicate a slight preference for vertical but most of the radar designs use horizontal. The choice is not clear. (Perhaps it doesn't matter?)

Critical Angle and Target Detectability. The difference in critical angle for the sea clutter and the target can result in the detection of clutter-limited targets at long ranges when it would be undetectable at shorter ranges. Figure 19 illustrates qualitatively why this can happen. The solid curve shows the approximate variation of the target echo signal with range, neglecting many factors such as the earth's curvature, refraction, interference lobes, and target cross section variation with elevation aspect. These are neglected to simply illustrate the gross nature of the phenomenon involved. The variation of the target echo with range before the critical angle is reached, is as R^{-4} as it should be for the classical radar equation. In the interference region below the critical angle corresponding to the target height, the variation is as R^{-8} . The sea clutter considered as a target has a cross section of $\sigma_c = \sigma^0 R \theta_b c(\tau/2) \sec \varphi$

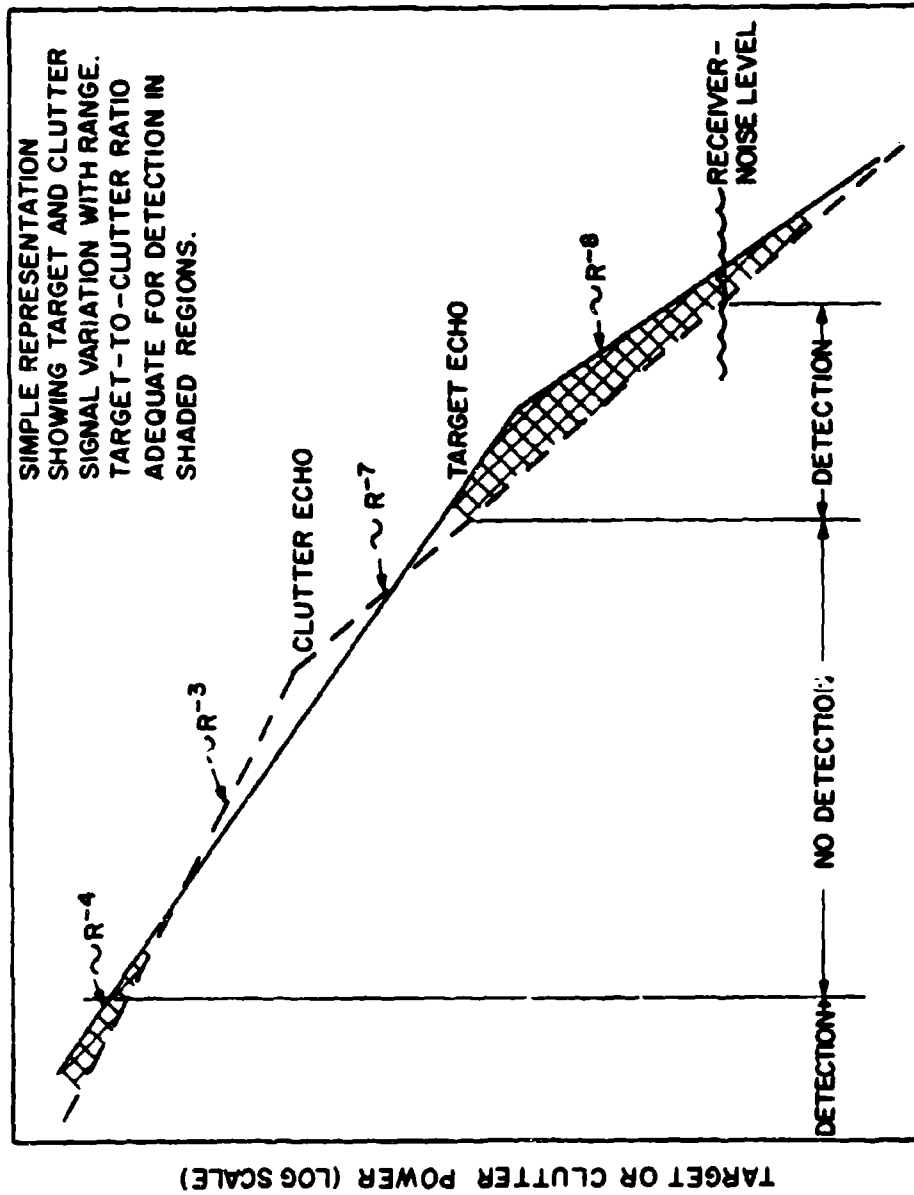


Fig. 19 - Simple representation showing target and clutter signal variation with range. The shaded regions indicate where the target-to-clutter ratio would be adequate for detection.

which when inserted into the classical radar equation gives a variation of R^{-3} at close range and at the longer ranges when the clutter lies below the critical angle, the variation is as R^{-7} . (Many factors have been omitted to illustrate the effect simply.) Figure 19 shows that at short ranges the target-to-clutter ratio can be sufficiently high for target detection. As the range increases, the target echo falls off faster (R^{-4}) than the clutter echo (R^{-3}) and the target-to-clutter ratio becomes too small for detection. As the range is increased still farther, the critical angle of the clutter is reached and the clutter decreases as R^{-7} . If the target is sufficiently high above the water so that it is not in the interference region, the clutter echo will drop below the target echo and detection will again take place. Detection will continue to occur with increasing range until the target is in the interference region and the curves again intersect or until the range is so great that the receiver noise is no longer negligible.

Clutter Matched Filter. Classical radar design calls for the use of a matched filter in the receiver to maximize the signal-to-noise ratio. The noise need not be restricted to the white, Gaussian characteristic usually assumed. Clutter can be considered as noise and the frequency response function $H_c(f)$ for the matched clutter filter has been shown by Urkowitz^{2a} to be

$$H_c(f) = \frac{k}{S(f)} \quad (19)$$

where k is a constant and $S(f)$ is the spectrum of the received signal, i.e., Fourier transform of the time waveform $s(t)$. Such filters maximize the signal-to-clutter ratio when receiver noise is negligible but when noise cannot be neglected there can be a loss in detectability as compared to a filter matched for the noise-limited waveform in the absence of clutter. Thus some compromise must often be made if a single clutter filter is to be used in the noise-limited case as well. Physically the matched clutter filter achieves its effectiveness against clutter by making the range resolution small. It seems that both the matched clutter filter and the matched filter for white, Gaussian noise can be of comparable performance against clutter if wideband waveforms are used. The matched filter for noise would be the preferred approach since it also does well in the absence of clutter.

The theory and analyses of optimum filtering, the Q-function, the ambiguity diagram and waveform synthesis for achieving target enhancement in the presence of clutter have been thoroughly studied in the literature.^{6a} The practical application of these theoretical concepts has been limited.

MTI. When the target motion is sufficiently different from the motion of the sea to separate the target echo from the sea echo on the basis of frequency differences, CW, MTI or pulse doppler methods may be employed for further increasing the target-to-clutter ratio over that obtained from the resolution in angle and range. The separation of an aircraft target echo from the sea echo by doppler filtering is a good way to eliminate the competing clutter. However, a slow moving ship might have a doppler shift close to that of the sea so that MTI or doppler processing would be difficult. The problem is even more difficult when the MTI radar is on a moving platform such as a ship. As far as is known, past MTI radar design has generally been conventional in that low-pass filtering is employed to eliminate clutter rather than the bandpass filtering as might be a better fit to the actual spectrum as mentioned in Sec. 6.

Decorrelation with Frequency. The echo from a distributed target such as sea clutter will fluctuate in amplitude as a function of frequency. The frequency must change by approximately the reciprocal of the pulse width for decorrelation of the echo amplitude. The return from an ideal point target is independent of the frequency. Therefore it has been suggested that target-to-clutter enhancement can be obtained by using pulse-to-pulse frequency agility. There are several methods for processing the signal to achieve the reduction in clutter but the basic principle is to filter the nonfluctuating from the fluctuating return.

The frequency agility technique performs signal processing in the video portion of the receiver after the phase information has been removed. It acts on the amplitude information only (noncoherent signal processing). The physical process that is employed to reduce the clutter relative to the point target is the equivalent of range resolution and employs bandwidth for this purpose just as the short pulse and the pulse compression radars do for reducing clutter. The classical short pulse radar also can be thought of as decorrelating the clutter. Its spectrum can be broken into a number of narrow intervals analogous to the different frequencies employed by the frequency-agile, clutter-decorrelation radar. Clutter is decorrelated except in the region corresponding to the reciprocal of the bandwidth. Thus the short pulse and pulse compression radars are cousins to the frequency agile radar. The usual frequency agile radar as referred to here performs its processing in the video and so will suffer more degradation at low signal-to-noise ratios than a short pulse or pulse compression radar with coherent (matched filter) predetection processing. The short pulse technique is also superior to the usual implementation of a noncoherent frequency-agile radar when viewing a large distributed target in distributed clutter. The short pulse radar can resolve the target and might even give an indication of its shape, without loss in detectability. The noncoherent frequency-agile radar on the other hand might process a distributed target just as it would distributed clutter and the target might be removed along with the clutter.

Another advantage of coherent methods is that it is known how to design such waveforms for good range and doppler resolution. The frequency agile radar might have an advantage in some limited situations if the bandwidth over which it operates is considerably greater than that which can be obtained by a coherent pulse compression or short pulse radar. In such a case there could be an equipment advantage for the wide-band noncoherent frequency-agile signal processing method. However, the state of the art in pulse compression is such that there are not many situations where a noncoherent frequency-agile, clutter-decorrelation radar would be the preferred means for enhancing the target-to-clutter ratio.

The Selection of σ° . One of the recurring messages made throughout this report is that the existing data for sea echo is not precise and is not completely related to a satisfactory theoretical model of the sea scattering mechanism or to oceanographic parameters. Nevertheless, the radar system engineer must have quantitative information on which to base design and has to use the best data he thinks is available even if it is lacking in accuracy. The designer needs to know of σ° its probability density function, its correlation with time and its variation over a period of time and with location. These can be determined in any specific situation but it is usually too expensive to obtain complete information in most circumstances. The radar designer must estimate these factors as best as possible from the existing data and apply a safety factor if circumstances permit this luxury. Often only the average or the median value of σ° is available and not too good a value at that.

The curves of Fig. 7 can be used as a basis for selecting a value of σ° for design purposes when no better information is available. These curves might apply for winds of 15 knots at microwave frequencies. To account for σ° at other wind speeds the critical angle should be changed as given by Eq. (6) with the data for wave height as given in Fig. 2. The curves in the plateau region should be raised or lowered by the values suggested in Sec. 3. The value of σ° at normal incidence for other wind speeds can be found from Fig. 8. With a little boldness, design values can be generated provided the data of Fig. 7 is not extrapolated too far and the degree of uncertainty in the data is properly understood. The designer should not come to believe that with repeated usage this information becomes more correct. It should always be kept in mind that existing sea echo data can be improved but that the engineer must do the best with whatever is available at the time it is needed. Figure 20 is an example of the results of this type of brash extrapolation for a wind speed of 30 knots. Such extrapolations should be used only when no other information exists.

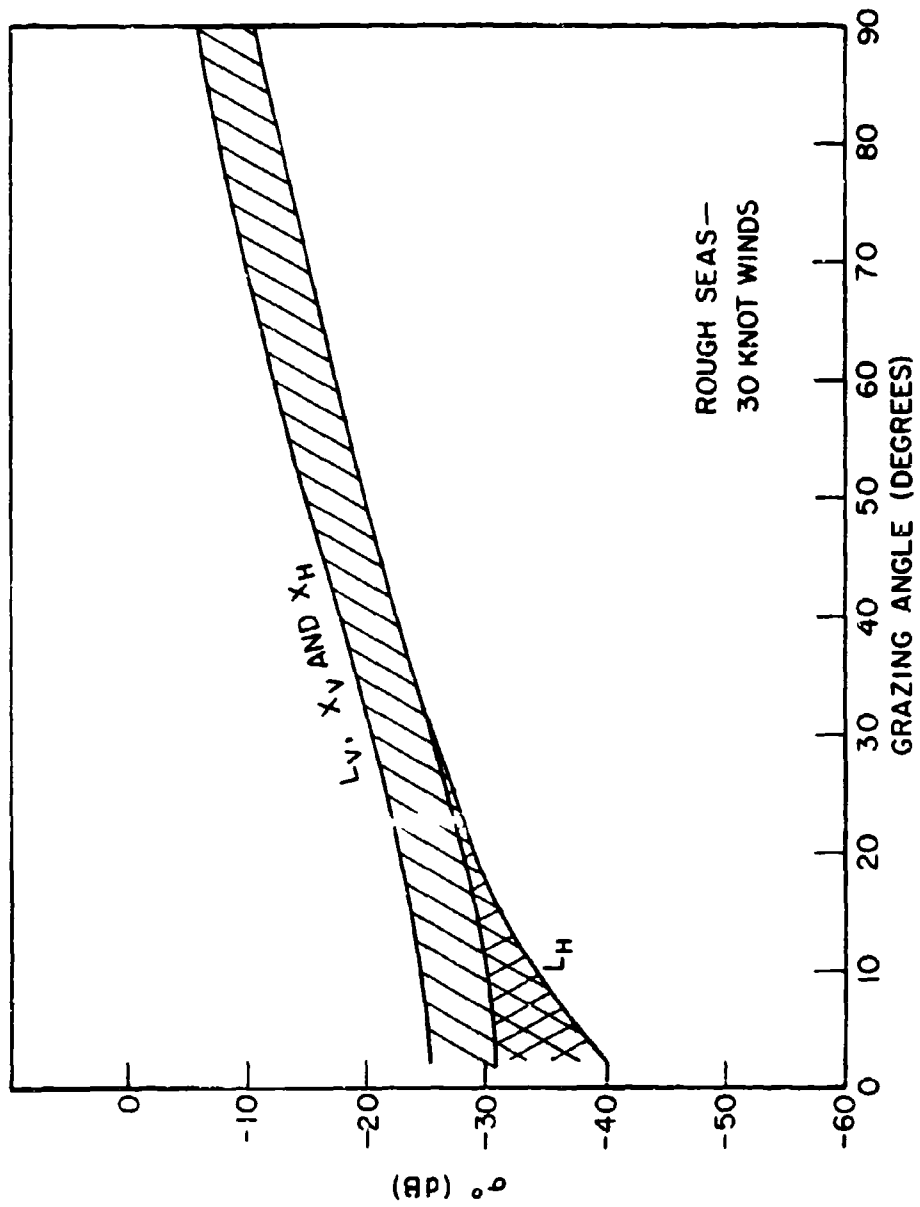


Fig. 20 - Extrapolated estimate of σ^0 for rough seas (about 30 knot winds) for microwave frequencies.

9. POTENTIAL OCEANOGRAPHIC APPLICATIONS

Radar sea echo is a nuisance to the radar designer who wants to maximize the ability to detect and track targets over the ocean. It is a form of interference that can limit the sensitivity of radar. However, sea echo can serve some useful purpose to the oceanographer, if not the radar designer. In recent years there has been increasing interest in applying radar for the measurement of oceanographic information. The oceanographic-measurement radar might be operated from land, ship or aircraft and serious consideration is being given to operation from satellites.

Of chief interest seems to be the use of radar to measure the roughness of the sea, or the sea state. Since the sea surface roughness is dependent upon the wind it is hoped that radar sea echo can give an indication of the local wind conditions as well as the roughness. The effect of wind on σ^0 vs grazing angle as in Figs. 6 and 7 illustrates several methods for measuring wind (or sea state) with radar. Consider the variation of σ^0 vs angle near normal incidence as illustrated in Fig. 21. The shape of this portion of the σ^0 vs ϕ curves depends on the wind. The scatterometer proposed by Moore and Pierson⁶⁷ is based on this principle. The scatterometer measures σ^0 vs grazing angle and relates the shape to the surface wind speed.

It might also be possible to correlate the absolute value of the echo at normal incidence with sea state. This would have the advantage, if it could be accomplished, of requiring the least power of any method for sea state measurement since σ^0 is at its maximum value at normal incidence.

In the plateau region the value of σ^0 depends on the wind and might be used to correlate radar with sea conditions. The variability of the data has generally been too great for serious attempts to take advantage of this correlation.

In principle, the critical angle can also be used to measure surface roughness. This would require much more power than the scatterometer because of the lower values of σ^0 at the critical angle, perhaps as much as 20 db or more.

Sea state might also be measured with high range resolution radar by examining the build up time of the leading edge of the pulse when viewing the sea at normal incidence. High range resolution combined with high angle resolution can actually profile the wave shape. Such radars probably would have to operate at the higher microwave frequencies, millimeter waves, or laser frequencies in order to achieve the necessary resolution.

Polarization ratio is also sea state dependent and might be useful if the variability in measurement is not excessive.

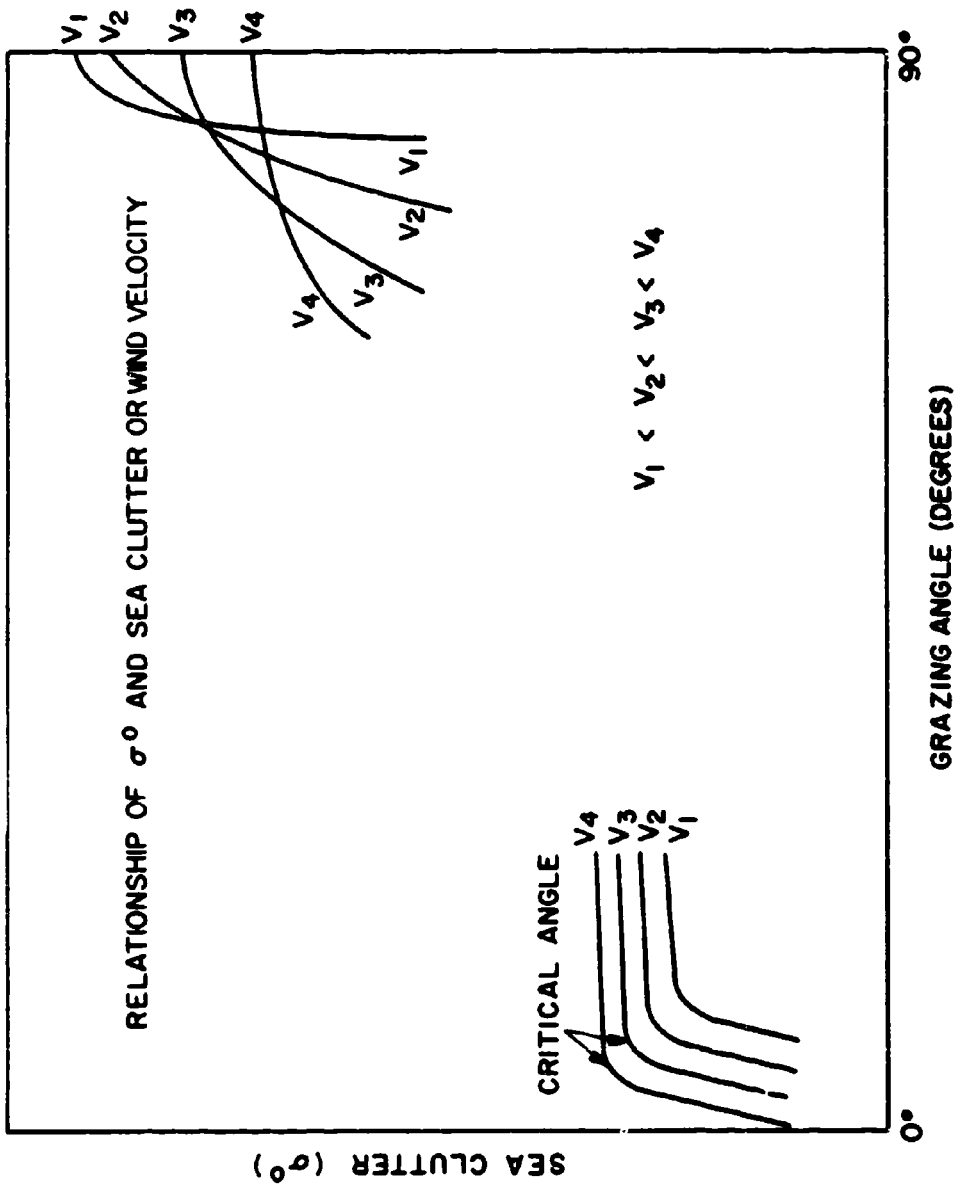


Fig. 21 - Relationship of σ° and wind speed, or sea clutter.

The sea echo from microwave radar at the lower grazing angles depends on the direction of the wind relative to the radar pointing direction. The echo is generally greatest looking into the wind and least looking with the wind. Measurements of σ^0 as a function of angle about a single observation point can then give the wind direction. This, however, is difficult to achieve.

The wind direction might also be obtained by comparing the magnitude of the two doppler frequency components corresponding to the approaching and receding resonant waves. (This correlation with wind has yet to be proven.) By measuring the amplitude of the doppler frequency components over a range of carrier frequencies, the ocean wave spectrum might possibly be obtained.

Water wavelengths and direction might be obtained by an imaging radar that can map the wave patterns. Imaging radars can also discern land-sea and ice-sea boundaries and can differentiate between different types of sea ice, if the dynamic range of the radar is adequate.

Microwave and millimeter radar might also be used to study the very small waves in the ocean. Present oceanographic techniques for studying the small capillary waves could be improved and radar is worth trying.

In addition to wave profiling, lasers operating at frequencies that can penetrate the water (blue-green) can also measure turbidity and do bottom contouring if the water is not too deep.

Measurement of the reflection coefficient of the sea over a range of frequencies under known sea-state conditions might be able to yield information as to the electrical properties of the sea, from which salinity might be inferred.

Although there seems to be many possible applications of radar to oceanography there has not been wide exploitation of radar for this purpose. Demonstration of feasibility would be required for almost all of the above mentioned techniques since most of these are still in the category of hopeful ideas rather than proven capabilities.

REFERENCES

1. Baker, B. B., Jr., Deebel, W. R., and Geisenderfer, R. D., (editors), "Glossary of Oceanographic Terms," 2nd Edition, 1966, U. S. Naval Oceanographic Office Special Publication SP-35, Washington, D. C.
2. Kinsman, B., "Wind Waves," Prentice-Hall, Inc., Englewood Cliffs, New Jersey, 1965.
3. Hogben, N., and Lumb, F. E., "Ocean Wave Statistics," London, Her Majesty's Stationery Office, 1967.
4. McLellen, H. J., "Elements of Physical Oceanography," Pergamon Press, New York, 1965.
5. Fairbridge, R. W., (Ed), "The Encyclopedia of Oceanography, Vol I," Reinhold Publishing Corp., New York, 1966.
6. Beckmann, P., and Spizzichino, A., "The Scattering of Electromagnetic Waves from Rough Surfaces," Pergamon Press, New York, 1963.
7. Goldstein, H., "A Primer of Sea Echo," U. S. Navy Electronics Laboratory, San Diego, California, Report 157, October 1949.
8. Long, M. W., Wetherington, R. D., Edwards, J. L., and Abeling, A. B., "Wavelength Dependence of Sea Echo," Final Report, Proj No. A-840, Georgia Institute of Technology, 15 July 1965.
9. Grant, C. R., and Yaplee, B. S., "Back Scattering from Water and Land at Centimeter and Millimeter Wavelengths," Proc IRE, Vol 45, pp 976-982, July 1957.
10. Macdonald, F. C., "The Correlation of Radar Sea Clutter on Vertical and Horizontal Polarization with Wave Height and Slope," 1956 IRE Convention Record, Vol 4, Part 1, pp 29-32.
11. Pierson, W. J., Jr., Neumann, G., and James, R. W., "Observing and Forecasting Ocean Waves," U. S. Naval Oceanographic Office, H. O. Publication No. 603, 1955.
12. Wright, J. W., "Backscattering from Capillary Waves with Application to Sea Clutter," IEEE Trans, Vol AP-14, pp 749-754, November 1966.
13. Kerr, D., (Ed), "Propagation of Short Radio Waves," Vol 13, MIT Radiation Lab Series, McGraw-Hill Book Co., New York, 1951.

14. Schooley, A. H., "Upwind-Downwind Ratio of Radar Return Calculated from Facet Size Statistics of a Wind-Disturbed Water Surface," Proc IRE, Vol 50, pp 456-461, April 1962.
15. Meyers, G. F., "High-Resolution Radar, Part IV - Sea Clutter Analyses," NRL Report 5191, October 21, 1958.
16. Macdonald, F. C., "Radar Sea Return and Ocean Wave Spectra," Proceedings of the Conference on Ocean Wave Spectra, Prentice Hall, pp 323-329, 1963.
17. Povejsil, D. J., Raven, R. S., and Waterman, P., "Airborne Radar," Van Nostrand Co., Inc., Princeton, New Jersey, 1961.
18. Goldstein, H., "Frequency Dependence of the Properties of Sea Echo," Physical Review, Vol 70, pp 938-940, December 1 and 15, 1946.
19. Daley, J. C., Ransone, J. T., Burkett, J. A., and Duncan, J. R., "Sea Clutter Measurement on Four Frequencies," NRL Report 6806, November 29, 1968.
20. Wiltse, J. C., Schleisinger, S. P., and Johnson, C. M., "Backscattering Characteristics of the Sea in the Region from 10 to 50 kMc," Proc IRE, Vol 45, pp 220-228, February 1957.
21. Jelalian, A. V., "Sea Echo at Laser Wavelengths," Proc IEEE, Vol 56, pp 828-835, May 1968.
22. Ament, W. S., Burkett, J. A., Macdonald, F. C., and Ringwalt, D. L., "Characteristics of Radar Sea Clutter: Observations at 220 Mc," NRL Report 5218, November 19, 1958.
23. King, A. M., Morrow, C. M., Myers, C. G., and Moody, C. L., "The Airborne Sea State Radar Principle and Preliminary Analysis of an Experimental Evaluation," NRL Memorandum Report 1884, June 1968.
24. Katzin, M., "On the Mechanisms of Radar Sea Clutter," Proc IRE, Vol 45, pp 44-54, January 1957.
25. Burrows, C. R., and Attwood, S. S., "Radio Wave Propagation," Academic Press, Inc., New York, 1949.
26. Bass, F. G., Fuks, I. M., Kalmykov, A. I., Ostrovsky, I. E., and Rosenberg, A. D., "Very High Frequency Radiowave Scattering by a Disturbed Sea Surface," IEEE Trans, Vol AP-16, pp 554-568, September 1968.
27. Schooley, A. H., "Some Limiting Cases of Radar Sea Clutter Noise," Proc IRE, Vol 44, pp 1043-1047, August 1956.

28. Urkowitz, H., "Filters for the Detection of Small Radar Signals in Noise," J. Appl. Phys., Vol 24, pp 1024-1031, August 1953.
29. Davies, H., and Macfarlane, G. G., "Radar Echoes from the Sea Surface at Centimeter Wavelengths," Proc. Phys. Soc., Vol 58, Part VI, pp 717-729, November 1946.
30. Long, M. W., "Polarization and Sea State," Electronic Letters, Vol 3, pp 51-52, February 1967.
31. Long, M. W., "On Polarization and the Wavelength Dependence of Sea Echo," IEEE Trans, Vol AP-13, pp 749-754, September 1965.
32. Daley, J. C., Ransone, J. T., Jr., Burkett, J. A., and Duncan, J. R., "Upwind-Downwind-Crosswind Sea Clutter Measurements," NRL Report 6881, April 14, 1969.
33. DeLorenzo, J. D., and Cassedy, E. S., "A Study of the Mechanism of Sea Surface Scattering," IEEE Trans, Vol AP-14, pp 611-620, September 1966.
34. Beckmann, P., "Shadowing of Random Rough Surfaces," IEEE Trans, Vol AP-13, pp 384-388, May 1965.
35. Brockelman, R. A., and Hagfors, T., "Note on the Effect of Shadowing on the Backscattering of Waves from a Random Rough Surface," IEEE Trans, Vol AP-14, pp 621-626, September 1966.
36. Findlay, A. M., "Sea-Clutter Measurement by Radar-Return Sampling," NRL Report 6661, February 12, 1968.
37. George, S. F., "The Detection of Nonfluctuating Targets in Log-Normal Clutter," NRL Report 6796.
38. Crombie, D. D., "Doppler Spectrum of Sea Echo at 13.56 Mc/s," Nature, Vol 175, pp 681-682, April 1951.
39. Steele, J. G., "Backscatter of Radio Waves from Progressive and Standing Waves in the Ocean," 1967 URSI Spring Meeting, Ottawa, Canada, May 23-26.
40. Ingalls, R. P., and Stone, M. L., "Characteristics of Sea Clutter at HF," IRE Trans, Vol AP-5, pp 164-165, January 1957.
41. Marks, W., "The Application of Airborne Radar Backscatter to Measurement of the State of the Sea, Oceanography from Space, Ref. No. 65-10, Woods Hole Oceanographic Institution, Woods Hole, Massachusetts, pp 377-391, April 1965.

42. Hicks, B. L., Knable, N., Kovaly, J. J., Newell, G. S., Ruina, J. P., and Sherwin, C. W., "The Spectrum of X-band Radiation Backscattered from the Sea Surface," J. Geophys. Res., Vol 65, pp 825-837, March 1960.
43. Wu, J., "Wind Stress and Surface Roughness at Air-Sea Interface," Hydronautics Incorporated, Technical Report 231-18, December 1967.
44. Neumann, G., and Pierson, W. J., Jr., "Principles of Physical Oceanography," Prentice-Hall, Inc., Englewood Cliffs, New Jersey, 1966.
45. Smith, B. G., "Geometrical Shadowing of a Random Rough Surface," IEEE Trans, Vol AP-15, pp 668-671, September 1967.
46. Cartwright, D. E., "Analysis and Statistics," Chapt 15 of "The Sea," Vol 1, M. N. Hill, Editor, Interscience Publishers, New York, 1962.
47. Barber, N. F., and Tucker, M. J., "Wind Wave," Chapt 19 of "The Sea," Vol 1, M. N. Hill, Editor, Interscience Publishers, New York, 1962.
48. Cote, L. J., et al, "The Directional Spectrum of a Wind Generated Sea as Determined from Data Obtained by the Stereo Wave Observation Project," New York University Meteorological Papers, Vol 2, No. 6, June 1960.
49. Moskowitz, L., "Estimates of the Power Spectrums for Fully Developed Seas for Wind Speeds of 20 to 40 Knots." J. Geophys. Res., Vol 69, No. 24, pp 5161-5179, 1964.
50. Cox, C. S., "Ripples," Chapt 21 of "The Sea," Vol 1, M. N. Hill, Editor, Interscience Publishers, New York, 1962.
51. Karaki, S., and Hsu, E. Y., "An Experimental Investigation of the Structure of a Turbulent Wind Over Water Waves," Stanford University Department of Civil Engineering, Technical Report No. 88, March 1968.
52. Communication from I. W. Fuller, NRL.
53. Trunk, G. V., "Noncoherent Detection of Nonfluctuating Targets in Contaminated-Normal Clutter," NRL Report 6858, March 21, 1969.
54. Trunk, G. V., "Median Detector for Noncoherent Distributions," NRL Report 6898, 1969.
55. Blair, J. C., Melanson, L. L., and Treten, L. H., "H.F. Ionospheric Radar Ground Scatter Map Showing Land-Sea Boundaries by a Spectral-Separation Technique," Electronics Letters, Vol 5, pp 75-76, 20 February 1969.

(Page 66 is blank)

56. Pidgeon, V. W., "Doppler Dependence of Radar Sea Return," J. Geophys. Res., Vol 73, pp 1333-1341, February 15, 1968.
57. Ament, W. S., "Forward and Back Scattering from Certain Rough Surfaces," IRE Trans, Vol AP-4, pp 369-373, July 1956.
58. Wright, J. W., "A New Model for Sea Clutter," IEEE Trans, Vol AP-16, pp 217-223, March 1968.
59. Valenzuela, G. R., "Radar Scattering from Rough Surfaces," Report of NRL Progress, pp 8-12, May 1968.
60. Barrick, D. E., and Peake, W. H., "Scattering from Surfaces with Different Roughness Scales: Analysis and Interpretation," Battelle Memorial Institute, Report No. BAT-197A-10-3, November 1, 1967.
61. Croney, J., "Improved Radar Visibility of Small Targets in Sea Clutter," The Radio and Electronic Engineer, Vol 29, pp 135-148, September 1966.
62. Deley, G. W., "Radar Waveform Design," General Research Corporation Technical Memorandum 843, June 1968, Sec 3.6.
63. Katzin, M., Bauchman, R. W., and Binnian, William, "3- and 9-Centimeter Propagation in Low Ocean Ducts," Proc IRE, Vol 35, pp 891-905, September 1947.
64. Harrison, A., "Methods of Distinguishing Sea Targets from Clutter on a Civil Marine Radar," The Radio and Electronic Engineer, Vol 27, pp 261-275, April 1964.
65. Corriher, H. A., Jr., Pyron, B. O., Wetherington, R. D., and Abeling, A. B., "Radar Reflectivity of Sea Targets," Vol 1, Georgia Institute of Technology, Final Report on Project A-914, 30 September 1967.
66. Hunter, I. M., and Senior, T. B. A., "Experimental Studies of Sea-Surface Effects on Low-Angle Radars," Proc IEE, Vol 113, pp 1731-1739, November 1966.
67. Moore, R. K., and Pierson, W. J., "Measuring Sea State and Estimating Surface Winds from a Polar Orbiting Satellite," Proc Symp on Electromagnetic Sensing of the Earth from Satellites, November 22-24, 1965, edited by R. Zirkind, Polytechnic Press.

UNCLASSIFIED
Security Classification

DOCUMENT CONTROL DATA - R & D		
<i>Security classification of title, body of abstract and indexing annotation must be entered when the overall report is classified</i>		
1. ORIGINATING ACTIVITY (Corporate author) Naval Research Laboratory Washington, D. C. 20390		2a. REPORT SECURITY CLASSIFICATION Unclassified
		2b. GROUP ---
3. REPORT TITLE A REVIEW OF RADAR SEA ECHO		
4. DESCRIPTIVE NOTES (Type of report and inclusive dates) A summary report.		
5. AUTHOR(S) (First name, middle initial, last name) Merrill I. Skolnik		
6. REPORT DATE July 1969	7a. TOTAL NO. OF PAGES 70	7b. NO. OF REFS 67
8a. CONTRACT OR GRANT NO. None	9a. ORIGINATOR'S REPORT NUMBER(S) NRL Memorandum Report 2025	
b. PROJECT NO.	9b. OTHER REPORT NO(S) (Any other numbers that may be assigned this report)	
c.		
d.		
10. DISTRIBUTION STATEMENT This document has been approved for public release and sale; its distribution is unlimited.		
11. SUPPLEMENTARY NOTES		12. SPONSORING MILITARY ACTIVITY None
13. ABSTRACT <p>The radar echo from the sea limits the ability of radar to detect targets. A knowledge of the sea echo is necessary, therefore, for proper design of radars that must detect targets on or over the sea. This report briefly reviews the ocean surface characteristics that affect radar echo and summarizes the present status of knowledge of the sea echo as a function of radar grazing angle, sea state and wind, polarization, frequency and other factors. A plot of σ^0 (radar cross section per unit area) as a function of grazing angle and frequency obtained from an averaged composite of reported data shows that no simple law of frequency dependence should be expected. The attempts made in the past to provide theoretical models describing the sea echo are reviewed and lead up to the presently accepted models of scattering surfaces composed of the larger gravity waves on which are superimposed the smaller capillary waves. The influence of sea echo on radar design is discussed and is considerably different than the usual design restraints imposed by thermal noise. The potential application of radar for oceanographic measurements such as sea state and wind is described.</p>		

DD FORM 1473 (PAGE 1)
1 NOV 68

S/N 0101-807-6801

67

UNCLASSIFIED
Security Classification

UNCLASSIFIED

Security Classification

14 KEY WORDS	LINK A		LINK B		LINK C	
	ROLE	WT	ROLE	WT	ROLE	WT
Sea clutter Radar Radar detection						

UNCLASSIFIED